CRAIOVA UNIVERSITY
FACULTY OF MECHANICS
DOCTORAL SCHOOL: Radu Voinea
FUNDAMENTAL FIELD: Engineering Sciences
FIELD: Mechanical engineering

DOCTORAL THESIS

CONTRIBUTIONS TO BIOMECHANICAL STUDY OF HUMAN WALKING

Scientific leader:
University professor PhD. eng. DANIELA TARNIŢĂ

Candidate:
PhD. eng. Petcu Alin Ionel

CRAIOVA
2019

CUPRINS

Chapter 1. Introduction, structure and objectives of the thesis

The aim and objectives of this thesis have as a starting point the biomechanical study of normal and pathological human walking on the ground and on the horizontal and inclined treadmill, but also the practical necessity of developing an optimized exoskeleton model for the recovery of the movements of the human lower limb joints, starting from the data gathered from specialist literature that highlight an alarming statistical increase in the incidence of articular osteoarthritis, a major chronic disease commonly found in the average and advanced age population, often leading to severe pain, adverse effects on quality of life, limiting mobility, increasing morbidity, and ultimately prosthetic surgery and unwanted effects.

The aim of the thesis is to study biomechanically normal and pathological human walking on the ground and on the horizontal and inclined treadmill, with application in the development of an exoskeleton device for the recovery of the movements of the human joints of the lower limbs. Starting from this general purpose, this thesis has the following specific objectives:

- Biomechanical study of human lower limb joint movements on samples of healthy subjects and patients, walking on the ground and on horizontal and inclined treadmill;
- Elaboration of the mathematical model of normal walking on the ground in order to obtain the laws of variation of the reaction forces with the ground;
- The realization of the virtual prototype and the physical prototype of the exoskeleton used to recover the movements of the human lower limb joints;
- Kinematic calculation of the exoskeleton;
- Numerical simulation of the walking of a virtual independent mannequin and, respectively, of the walking of a mannequin assisted by the exoskeleton proposed in the thesis.

After a brief presentation of the objectives and purpose of the thesis in **Chapter 1**, **Chapter 2** presents the main elements of anatomy of a human inferior member, as well as the main elements of the biomechanics of human lower limb joints.

Chapter 3 presents the recent state of the research on biomechanical analysis of human walking as well as devices such as orthoses and exoskeletons used in the medical recovery of human lower limb joint movements.

Chapter 4 shows the biomechanical evaluations of lower limb joints in both healthy subjects and patients affected by knee osteoarthritis, before and after the prosthesis.

Chapter 5 presents the development of a mathematical model of the human motion on the ground in order to numerically determine the rectifying forces of the ground in time of the human walking.

Chapter 6 presents the development of the virtual model of the exoskeleton recovery device proposed in the doctoral thesis in order to ensure the recovery of flexion-extension movements of the lower limb joints.

Chapter 7 is dedicated to the cinematic and dynamic analysis of both human and exoskeleton walking using ADAMS software. The chapter begins with defining the virtual model of the mannequin and the mass properties required for simulation.

Chapter 8 presents the dissemination of the research results of the doctoral thesis, the original contributions of the author, as well as the future research directions in the field of research approached.

Chapter 2. Elements of anatomy and the biomechanics of human walking

Hip joint is a spherical joint with three axes of movement, with great movement and locomotion. This joint is made up of the coxtail acetabulum and the femoral head. The articular faces are represented by the head of the femur and the half-face of the acetabulum [MS2007], [VP2003], [MP1998].

Knee joint is the most complicated joint in the human body. Three bones take part in it: the femur, the patella and the tibia. It has a biarticular structure: tibiofemoral and patellofemoral articulation. It is subjected to large forces occurring both during the transmission of human body weight in statics and during the action of torque forces required for locomotion [MP1998].

Talocrural joint, called the ankle joint, joins the two bones of the ankle with the talus and forms a typical trochlear articulation. It is a joint formed by the articular faces of the distal epiphyses of the tibia and the fibula with the articular faces of the astragal. This is the lower link of the triple extension chain. Ensures that the foot is horizontal, forming a stable platform capable of transmitting body weight to the ground. It plays an important role in walking performance by lifting the heel and pushing the center of gravity of the body forward into plantar flexion [MS2007], [VP2003], [MP1998]

2.3. Elements of human walking biomechanics

Human body locomotion represents any form of walking, running, jump, climbing and is done by the bone, joint and muscle system. Inertial, gravitational, muscle, reaction forces are involved in this process of locomotion.

The simplest way of locomotion is walking, which consists in the successive alternative movement of the lower limbs, which have the role of support and propulsion. The main feature of walking is to support the body with the surface of the ground, either with one foot or both. The successive movement of one member towards each other represents a cycle, being the corresponding period of time between the two contacts of the heel with the ground. During one walking cycle, there are two single support periods (each of about 40% of the walking cycle) and two short double support periods when the center of gravity of the body is in the lowest position.In one specialized works, the authors divide the walking cycle into a number of 8 phases - figure 2.10: initial contact, loading response, midstance, terminal stance, pre-swing, initial swinging, midswing, terminal swing, [JP 2010] Instead, in other works, the authors divide the course in just 7 or 6 phases - Figure 2.11. [LAL2015].

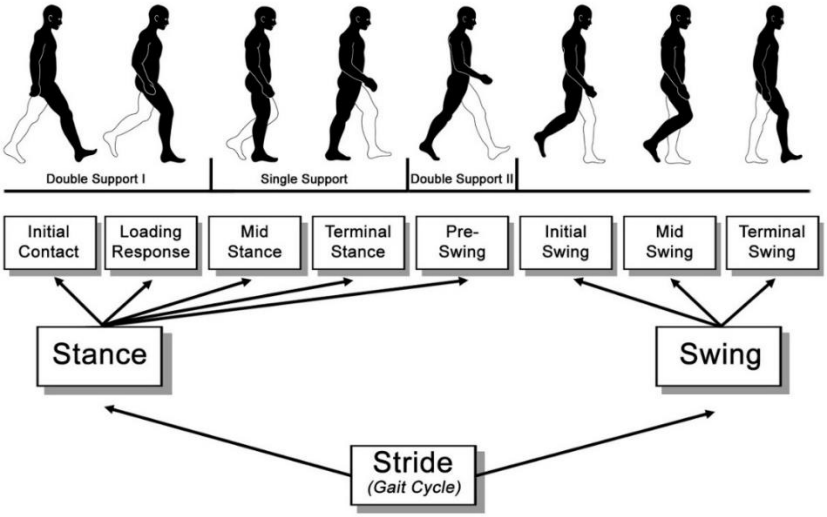

Fig. 2.10. 8-phase walking cycle [JP 2010]

Biomechanics of hip joint (coxofemoral)

The hip joint is the upper link of the triple extension chain, having an important role in the posture of the human body. The following movements are made at this joint level: flexion-extension, abduction-adduction, rotation and circumduction. Due to the length of the femur and the inclination angle, the flexion-extension movements and the abduction-adduction movements are associated with rotational movements [VP2003], [MP1998].

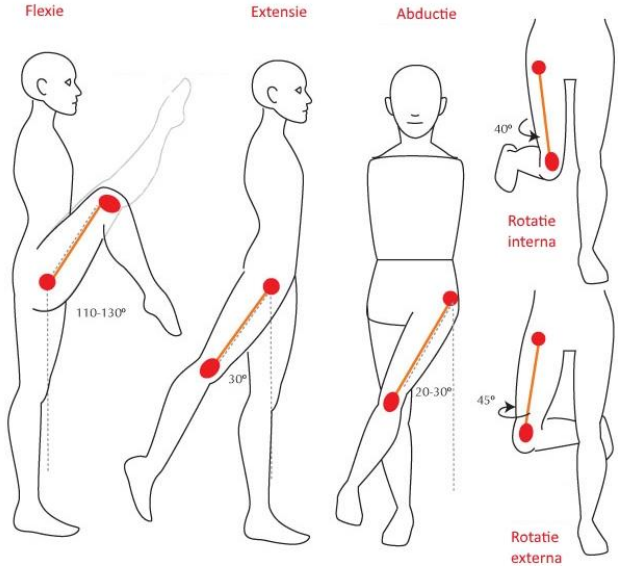

Fig. 2.19. Hip joint movements: flexion-extension, abduction-adduction, internal rotation-external rotation [WCLG]

Biomechanics of the knee joint

The joint of the knee allows the transmission of the human body weight both in motion and static. It is a single axle joint, the two main movements shown in Figure 2.20 that can be executed are flexion and extension. The secondary movements that can be produced in the knee joint are those of the medial and lateral rotation. Although very small in amplitude, marginal, medial and lateral tilt movements can also occur in this joint.

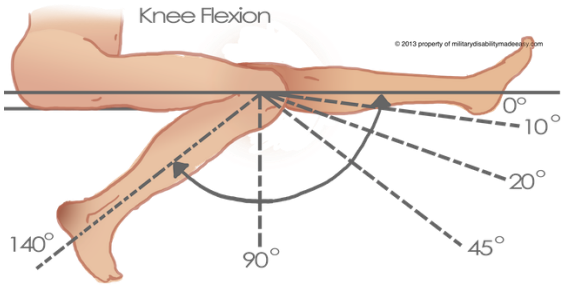

Fig. 2.20. Maxim angle achieved during flexion-extension [SKMO]

Biomechanics of ankle joint

The ankle joint is characterized by the following movements: dorsal flexion-extension, abduction, adduction, circumduction, supination, and pronation.

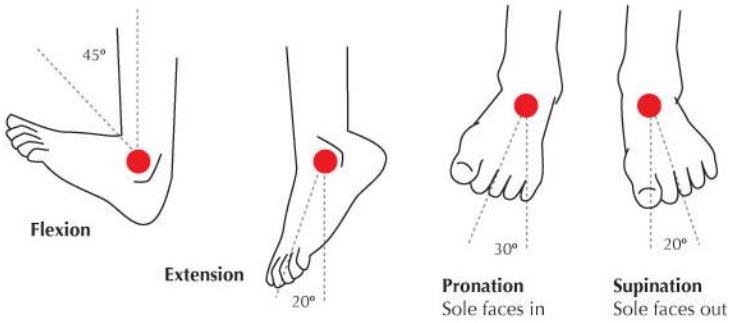

Fig. 2.21. Ankle joint movements: flexion-extension, pronation-supination [WCLG]

Chapter 3. The state-of-the-art research on systems for medical recovery

3.1. Introduction

Nowadays, the importance of measuring and analyzing walking variability has increased and is increasingly recognized and used in biomechanics and clinical research. Clinical walking analysis usually consists of measuring walking parameters, kinematic analysis, kinetic measurement and electromyography. Space and timing parameters provide useful information for diagnosis and therapeutic action [BRK1989]. In the medical field, knowing walking characteristics, monitoring and assessing changes in human walking, reveals important information about quantitative objective measurement of walking parameters and early evolution and diagnosis of various diseases [MDLH2014, SDH2001, SDH2002, SDH2005, WT2012, CF2014].].

3.2. Orthosis

The orthosis represents the device attached externally to a part of the body in order to prevent the occurrence of a condition, to recover and correct after surgery, or to improve the movement of a part of the body. There is a wide range of types of orthotics on the market, from textile materials used for mild illnesses to rigid ones made from composite materials with electric or pneumatic drives used in postoperative recovery.

3.2.1. Passive orthoses

A passive orthosis is the device applied to a segment of the human body in order to correct or improve the function it serves or to reduce the symptoms of a disease. The orthesis is an externally applicable device that acts as a support or assists the neuromuscular-scheletic system. Fixed orthoses are of different shapes and are made of various materials. Some of these are custom made for each user. Others are manufactured for a sample of patients in different sizes (small, medium and large). All aim primarily at improving locomotor function and reducing tensions that cause pain or deformity.

3.2.2. Active orthosis

Active orthosis is the portable device that can be attached to the body and can support, take up weight and impose movement on the body area where it is attached. The construction of the active orthosis is much more complex, in addition to the orthosis structure, it also has an operating system that differs from case to case.

These devices are designed to help people with disabilities, people who have suffered a stroke or people who suffer from a member's injuries. They can be useful in the recovery and improvement of locomotor functions.

By using an active orthosis the stresses on the orthogonal limb decrease, and the patient's energy consumption during the movement can be optimized, which is useful to patients especially during the postoperative period [TY2009, AMD2008, JMF2011].

3.2.2.1. Electric drive systems

The use of electric motors offers two possibilities of actuation, a direct drive shown in Figure 3.7, when the electric motor axis forms a common axis with the joint axis, and an indirect actuation shown in Figure 3.8, by using a power transmission system. The electric drive system is most often used in orthogonal active systems and exoskeleton systems due to increased movement control, high torque ratio, low noise produced during operation and variety of sizes and power models in different configurations.

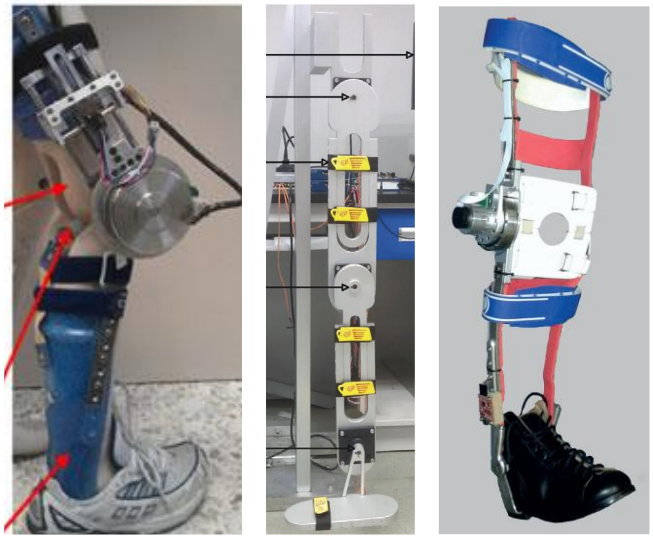

c) d) e)

Fig. 3.7. c) ATLAS knee [MC2015]; d) the lower limb rehabilitation robot type 3DOF [WJ2016]; e) Robotic orthosis [FL2016].

3.2.2.2. Pneumatic drive systems

In a pneumatic drive system, the main equipment is the pneumatic cylinder. It is used in most applications, taking into account advantages such as: the stroke of the piston is constant; due to the compression characteristics of the air, the pneumatic cylinder can attenuate shocks; has increased safety in use due to its simple and robust construction.

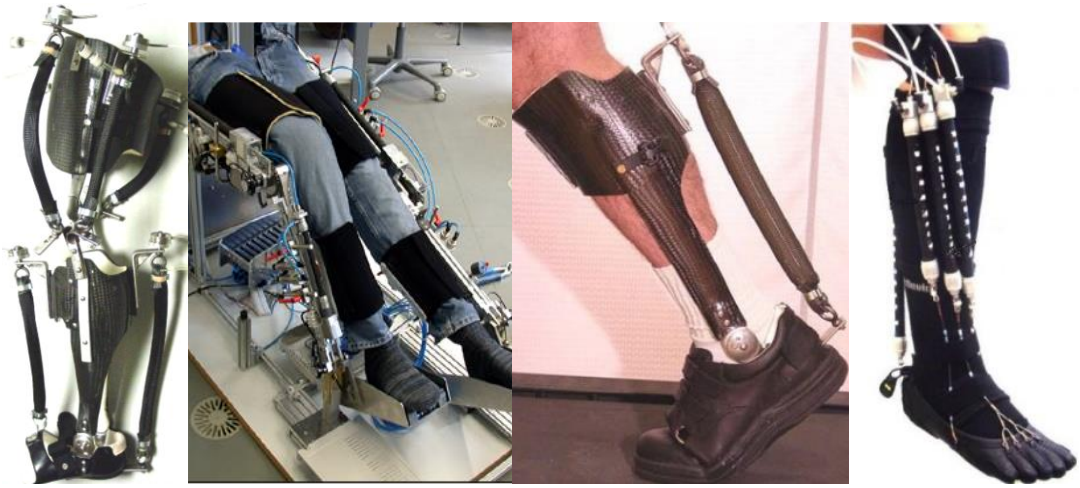

a) b) c) d)

Fig. 3.9. a) KAFO [GSS2009]; b) Bio-inspired orthoses [YLP2011]; c) Rehabilitation robot [MK2008]; d) AKAFO [SMC2007].

3.2.2.3. Hydraulic drive systems

The hydraulic drive system is especially used to operate the orthotics performing the load transfer function shown in figures 3.10. This drive system is recommended for use in heavy duty systems due to high torque, but it also has the disadvantage of the weight of the equipment, which can make the system difficult to carry. To reduce weight and energy consumption, but to maintain performance, have been developed hydraulic-electric hybrids to replace the classic hydraulic system.

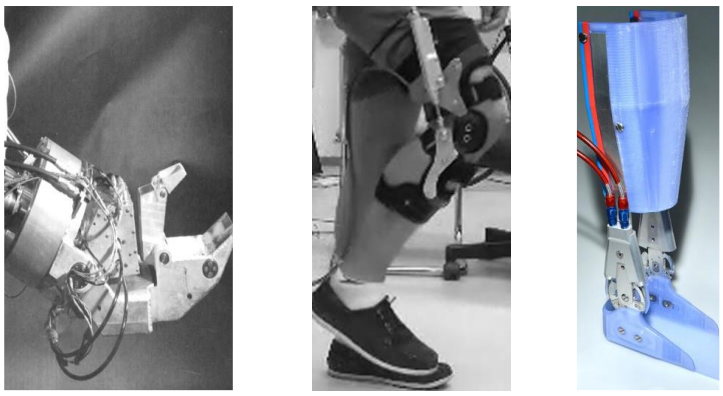

a) b) c)

Fig. 3.10. a) Orthosis Hardiman [BJM1971]; b) Orthosis KFO [MS2015]; c) Orthosis AFO [BCN2014];

3.3. Devices used to transfer the load

These devices are characterized by the ability to pick up and transfer body weight to the ground

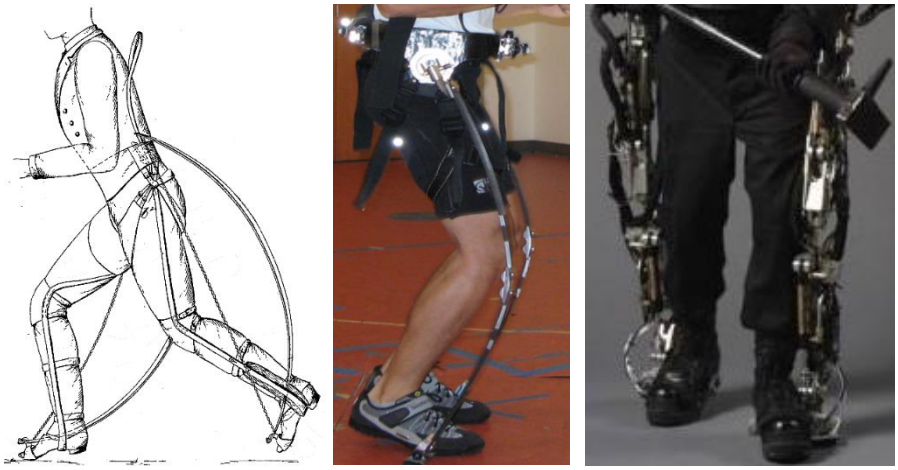

a) b) c)

Fig. 3.11. 3.11. Exoskeleton systems used for load transfer: a) N. Yagn patented exoskeleton [YN1890], b) Reinterpretation of N. Yagn patented exoskeleton by MIT Biomechatronics Group [AMG2009], c) Bleex Exoschelet [HK2006]

Chapter 4. Biomechanical evaluations of normal, osteoarthritic and prosthetic human knee joint

4.1. Introduction

Clinical walking analysis usually consists of measuring walking parameters, kinematic analysis, kinetic measurement and electromyography. Spatial parameters and walking time parameters provide diagnostic and therapeutic useful information if measurements are made accurately and with accurate equipments [BEG1989]. In the medical field, knowledge of walking characteristics, monitoring and assessing changes in human behavior reveal important information about the objective quantitative measurement of walking parameters and the early evolution and diagnosis of various diseases (MUR2014, SUT2001, SUT2002, SUT2005, TAO2012, CAS2014).

A large number of studies demonstrate the advantages, accuracy and validity of mobile sensors that can be worn by the subject to measure and analyze various parameters of normal or pathological human walking. Research papers studied healthy subjects [DAN2015, KUN2011, SAL2013] or were performed to evaluate the outcome of surgical procedures [KAN2012, KUR2007] or to identify movement kinematic differences in patient populations, such as patients with osteoarthritis [TAR2014 (ADC2005), patients with Parkinson's disease [JOL2012], prosthetic patients, compared to healthy subjects. The objective tracking techniques are based on the use of different devices to capture and measure information on different walking parameters [TAO2012].

4.2. Data acquisition systems

Biometrics

Echipamente integrate pentru analize complexe 3D ale omului de mers pe jos **Biometrics** [WBIOM] permite compilarea simultană a datelor biomecanice cinematice și dinamice prin intermediul unor electrogonometre, accelerometre, platforme de forță, senzori EMG, senzori de presiune de contact și alte tipuri de senzori sau echipamente care face parte din sistemul de achiziții publice. Un total de 24 seturi de date biomecanice perfect sincronizate pot fi achiziționate simultan prin canale de date analogice și digitale.

Electrogoniometers

Biometrics has a wide range of goniometers and torsiometers, which are ideal for fast, simple and accurate measurement of motion across multiple planes. Extremely robust, lightweight and flexible, the sensors can be comfortably worn under the clothing, without hindering the actual movement of the joint.

The SG goniometers series shown in Figure 4.1. (SG65, SG75, SG110, SG110/ A, SG150, SG150/ B) is used for simultaneous measurement in two planes. For example, to measure wrist movement, an SG65 goniometer is attached to the dorsal surface using double-sided adhesive tape. One end of the goniometer is positioned next to the third metacarpian, and the other end, across the median line of the forearm, with the wrist in a neutral position.

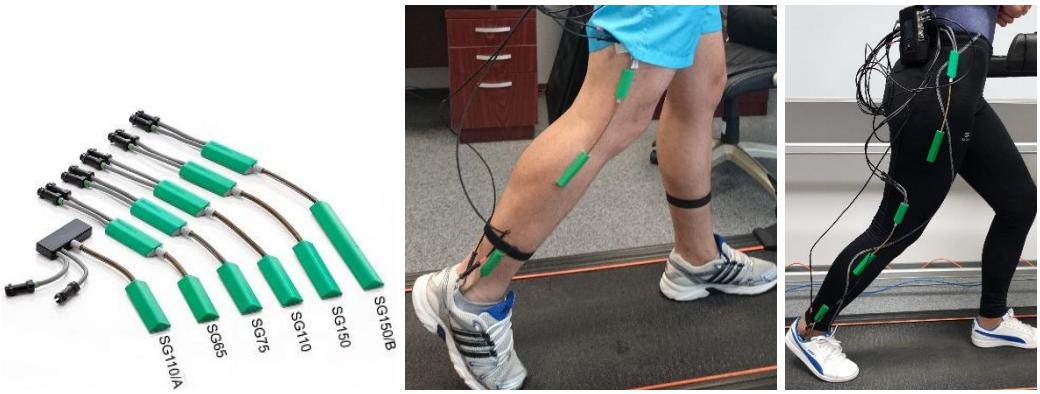

Fig. 4.1. SG goniometer series

Force platforms

Biometrics family force platforms have been designed for users' needs, providing high precision and ease of use. They can connect directly via Bluetooth to dataLINK and DATAlog systems for capturing experimental data and analyzing reaction force from a wide range of applications. These are used in walking analysis to measure the values of the reaction forces recorded on the contact between the feet and the ground in order to plot the variation graph of the reaction forces during a running cycle or several consecutive cycles and to determine the maximum values of them.

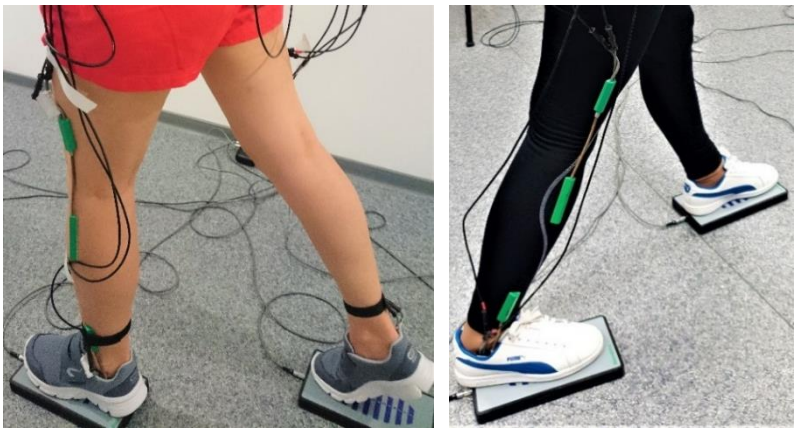

Fig. 4.2. Subjects with electrogoniometers and force platforms during experimental tests

DataLOG MWX8 [WBIOM]

DataLOG MWX8, shown in Figure 4.3., is a device that incorporates the latest data acquisition technology developed to meet data collection needs and portable monitoring of human performance in sports, medical research, industrial ergonomics, and research in education. It is a portable, lightweight device that can be attached to the body without interfering with data collection. Weighing very little (129g), the DataLOG MWX8 can also be worn on the arm or leg, compared to traditional belt/ waist placement.

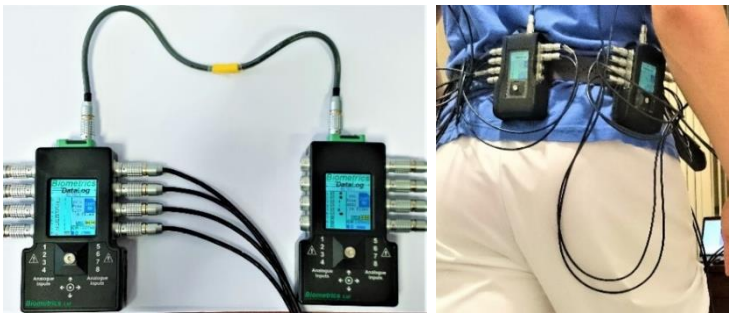

Fig. 4.3. The DATAlog MWX8 equipment

The equipment used during the tests consists of the following components:

- 2 electrogonometers SG 110 (Biometrics Ltd), mounted as shown in Figure 6.4. with the purpose of measuring the angles of flexion-extension and eversion-inversion of the ankle joint from the lower limbs;
- 4 electrogonometers SG 150 (Biometrics Ltd), mounted as shown in Figure 6.5. with the purpose of measuring flexion-extension and rotation angles in the knee and hip joint front plane of both lower limbs;
- 6 force platforms type FP 4 (Biometrics Ltd) mounted as shown in figure 6.7;
- 3 DataLOG (Biometrics Ltd UK), 2 for the 6 electrogonometers, ie 12 channels used, and 3 for all power platforms, ie 6 channels used.

4.3. The experimental protocol

Healthy subjects and patients

For the study were selected 17 persons grouped in 2 samples:

Healthy subjects sample - composed of 14 people, of which 8 male subjects and 6 female subjects.

Patient sample - composed of 3 subjects with knee osteoarthritis, of which 2 female patients and 1 male patient.

Table 4.1. Anthropometric data of the subjects

Subject	Sex	Age	Weight [Kg]	Height [cm]	Lower limb length [cm]	Length hip-knee [cm]	Length knee-ankle [cm]
Subject 1	M	26	79	185	90	46	44
Subject 2	F	27	55	168	71	36	35
Subject 3	M	26	71	179	85	43	42
Subject 4	F	28	53	165	69	35	34
Subject 5	M	26	75	182	89	46	43
Subject 6	F	30	53	162	68	35	33

Subject 7	M	26	73	178	86	44	42
Subject 8	M	30	80	181	89	45	44
Subject 9	M	26	82	182	90	46	44
Subject 10	F	27	54	167	70	36	34
Subject 11	M	26	75	180	86	44	42
Subject 12	F	26	56	169	71	37	34
Subject 13	M	26	83	180	87	45	42
Subject 14	F	26	53	162	68	35	33
Average		26,86	67,29	174,29	79,93	40,93	39
StdDev		1,46	12,50	8,27	9,52	4,83	4,72
Cv [%]		5,44	18,58	4,74	11,91	11,79	12,11

Patient sample

Three patients with knee joint disease were selected. During the collection of the data needed for the study, the patients were hospitalized at the Department of Orthopedics at Craiova County Emergency Hospital in order to prepare for prosthetic surgery at the level of the knee joint. In Table 4.2. the age and anthropometric data of the patients are presented.

Table 4.2. Anthropometric data of patients

Subject	Sex	Age	Weight [Kg]	Height [cm]	Lower limb length [cm]	Length hip-knee [cm]	Length knee-ankle [cm]
Patient 1	M	63	77	171	83	42	41
Patient 2	F	58	72	170	81	42	39
Patient 4	F	59	73	167	79	40	39
Average		60,00	74,00	169,33	81,00	41,33	39,67
StdDev		2,65	2,65	2,08	2,00	1,15	1,15
Cv		4,41	3,58	1,23	2,47	2,79	2,91

Experimental tests

Tests were performed using the Biometrics system.

Healthy subjects performed 23 different ground and mobile walking tests, of which 3 track tests with different speeds and 20 mobile walks with different speeds and inclinations. In Table 4.3. the tests performed by healthy subjects on the treadmill are presented. The tests performed by the subjects were carried out in the Laboratory of Biomechanics Research within the Research Platform of the University of Craiova, INCESA.

The 23 tests (T) are:

- Test 1 (T1) - running on the ground on a platform with a slow speed of approximately 0.4 m/ s;
- Test 2 (T2) - running on the ground on platforms with a normal speed of approximately 0.5 m/ s;
- Test 3 (T3) - Walking on the ground on a platform with a fast speed of about 0.67 m/ s.

Table 4.3. Tests run by healthy subjects on the treadmill

	0°	**3°**	**7°**	**11°**	**15°**
2,5 km/h	Test 4 (T4)	Test 5 (T5)	Test 6 (T6)	Test 7 (T7)	Test 8 (T8)

5 km/h	Test 9 (T9)	Test 10 (T10)	Test 11 (T11)	Test 12 (T12)	Test 13 (T13)
7,5 km/h	Test 14 (T14)	Test 15 (T15)	Test 16 (T16)	Test 17 (T17)	Test 18 (T18)
10 km/h	Test 19 (T19)	Test 20 (T20)	Test 21 (T32)	Test 22 (T22)	Test 23 (T23)

Because of the condition they suffered and the pain associated with this condition, patients with advanced osteoarthritis could not pass all the tests on the moving tape. They performed the T1, T2, T3, T6 and T11 tests at the County Emergency Hospital in Craiova both before and two months after the surgery.

4.4. Stages of collection and processing of experimental data

4.4.1. Collection of the data

The data collection process is simple, the subject-mounted electrogoniometers and power platforms transmit data via the cables to DataLog and the DataLOG converts the received signal and sends it via Bluetooth to the PC, all done in real time. The block diagram of the data acquisition process is shown in Figure 4.8.

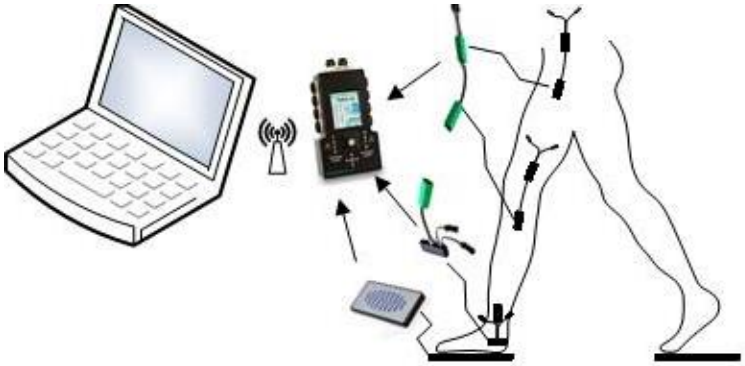

Fig. 4.8. The block diagram of the data acquisition process

Data received from the PC is converted by the Biometrics DataLOG software into charts. An example of variations in flexion-extension angle and angles of rotation in the front plane for the hip, knee and ankle joints of both lower limbs of a healthy subject represented by the software based on the experimental data collected is shown in Figures 4.9.

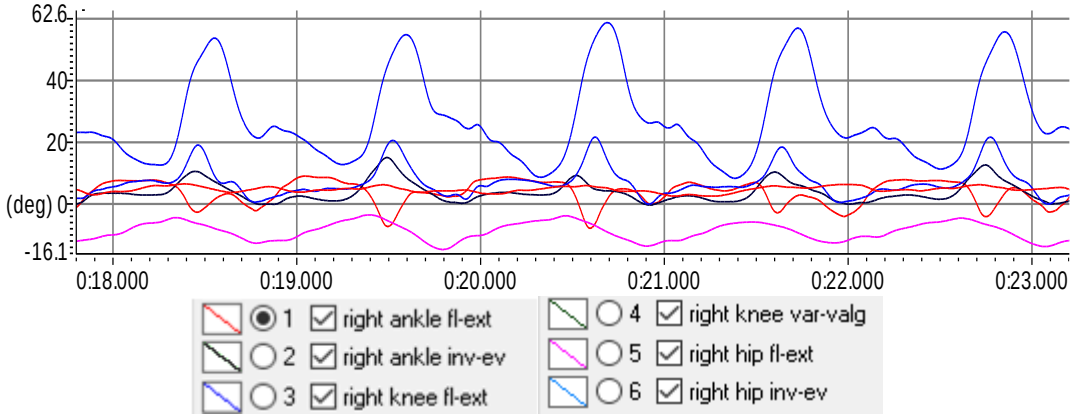

a)

Fig. 4.9. Diagrams of consecutive cycles of variation of flexion-extension angles in sagittal plane and rotation in the front plane represented by the software based on experimental data collected for the hip, knee and ankle: a) Right lower limb;

4.4.2. Data processing

For data processing, the SimiMotion software was used to import the experimental data files collected with the Biometrics data acquisition and processing system in .txt format, as well as their processing. Data processing in SimiMotion results in the average normalized cycles corresponding to each processed data file.

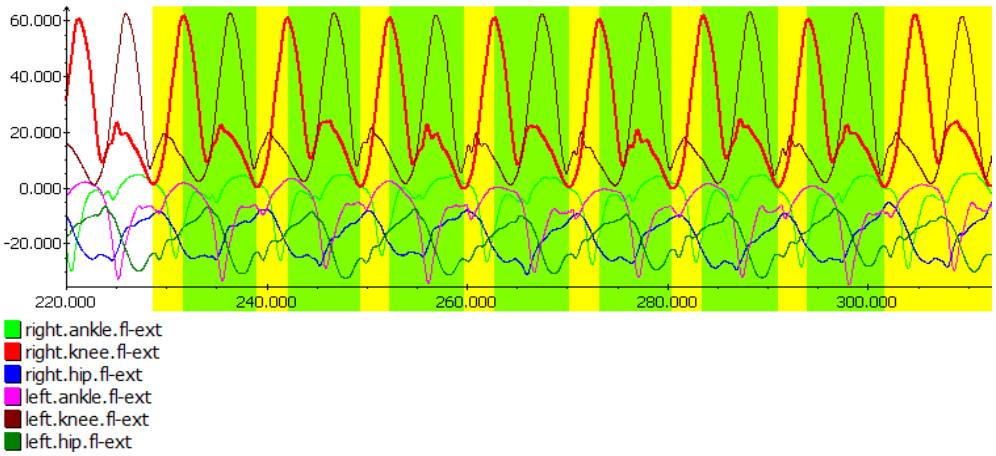

Fig. 4.14. Defining the interval used for phasing division

The next step in processing experimentally collected data is to calculate the average cycle using the Cut Into Phases command in the Project application. The result obtained is the average cycle of the consecutive cycles selected for walking analysis along with the corresponding Mean + StdDev and Mean-StdDev curves.

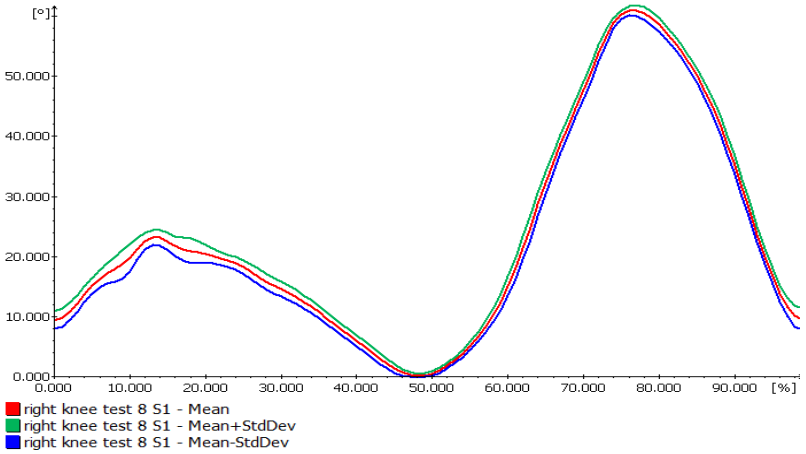

Fig. 4.14. Example of SimiMotion result chart for Average (mean), Mean + StdDev, Mean - StdDev cycle.

4.5. Results of the healthy subjects

Through all the steps of processing the data obtained from the measurements performed during the tests, the average cycles for the six lower limb joints were obtained for all healthy subjects. In figures 4.14. - 4.16. the middle flexion-extension angles of the six lower limb joints of subject 1 for the T4, T8 and T10 tests are presented. Similar charts were obtained for each test performed by each subject.

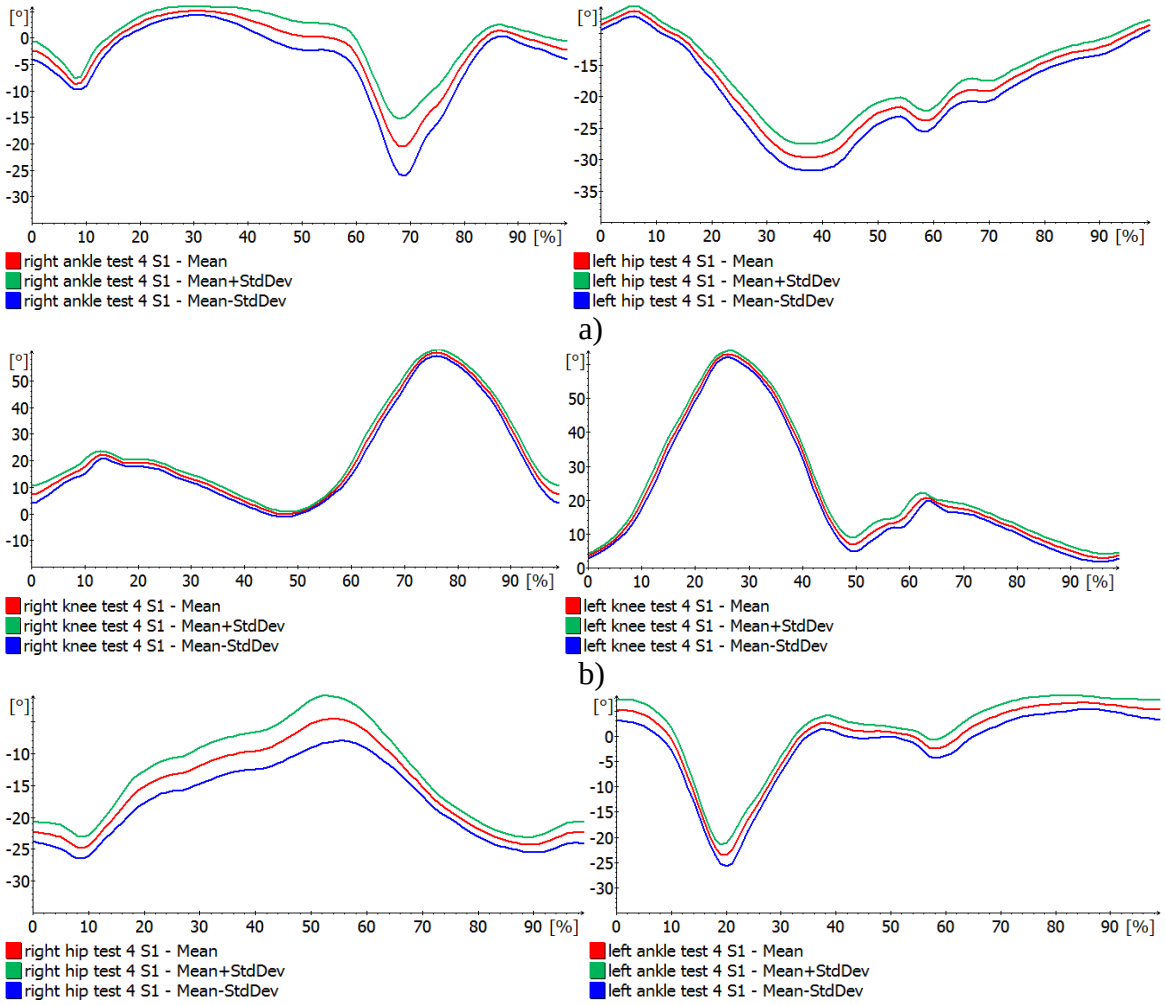

Fig. 4.14. Mean cycle, Mean cycle + StdDev, Mean cycle - StdDev cycle for a) Ankle joint, b) Knee joint, and c) Right and Left lower right hip joint - Subject 1 - Test 4

In Figure 4.17. the average cycle for test 4 for the lower right member at the sample level.

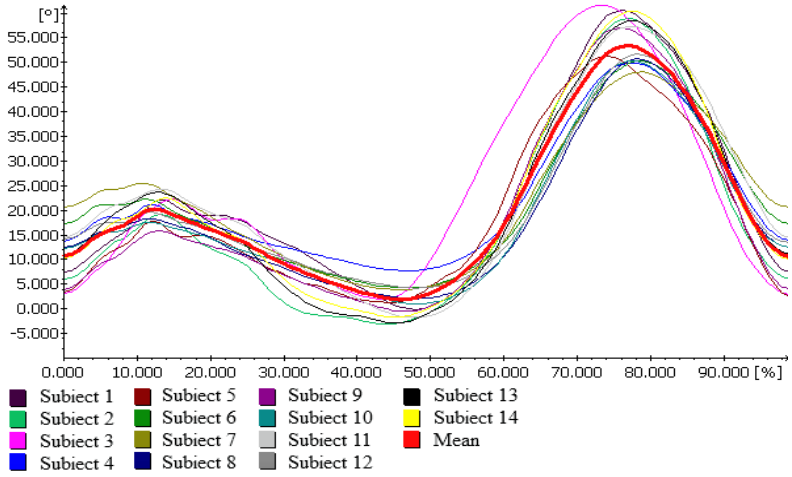

Fig. 4.17. The average cycles of each subject and the Mean cycle of the healthy sample for right knee, Test 4

In Figures 4.18. - 4.20. the comparative diagrams of the average cycles of the healthy sample are presented.

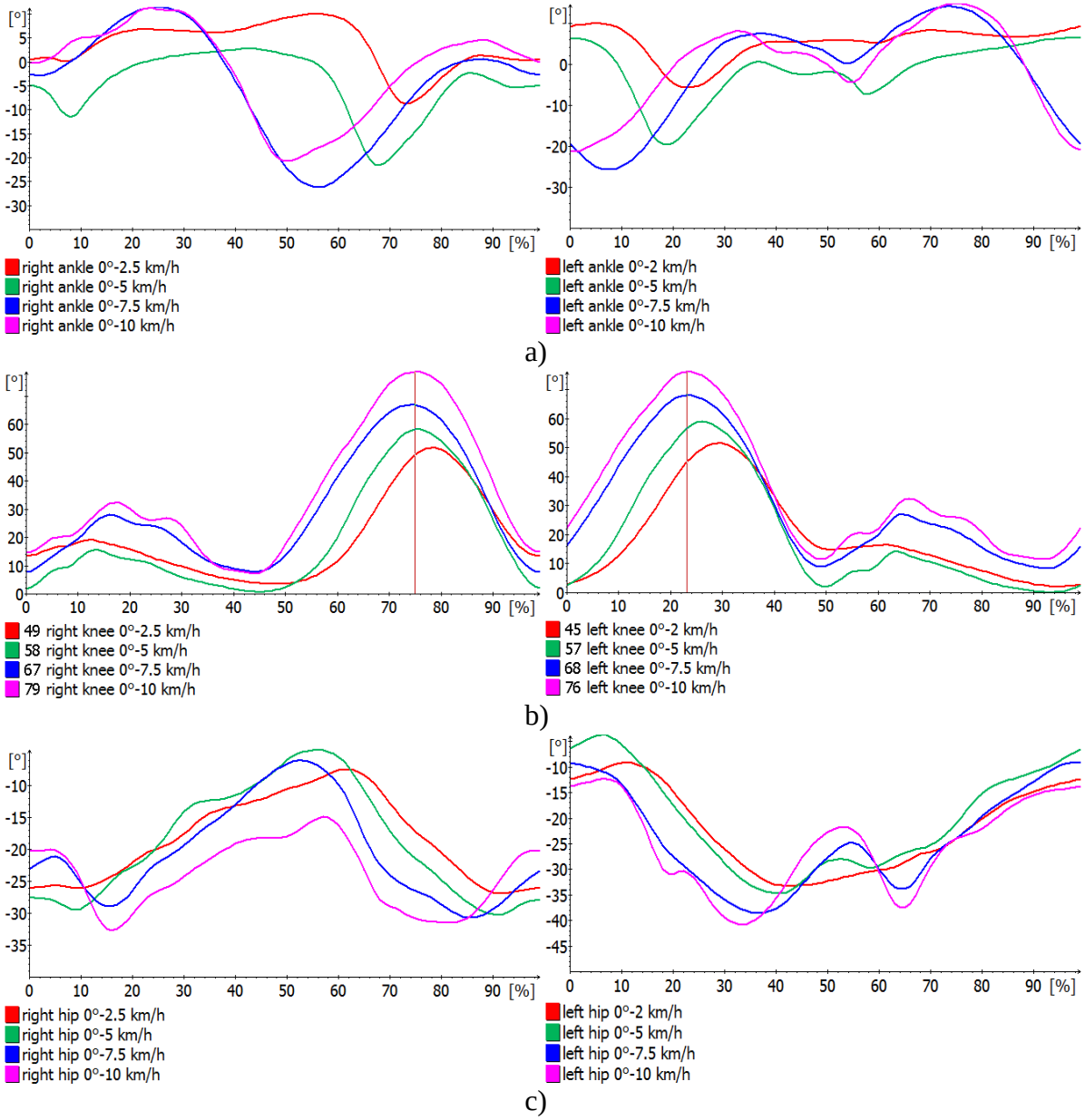

Fig. 4.18. Comparison between experimental Mean cyles for the a) ankle joint, b) knee joint, and c) left

4.5.1. Reaction forces

Simultaneously with the collection of data corresponding to the flexion-extension movement at the six joints, experimental data from 6 force platforms for the first 3 tests on the surface of the ground were collected for both subjects and patients. Charts of experimental reaction forces, based on experimental data collected from the force platforms, corresponding to healthy subjects, are found in Figures 4.25. - 4.28.

In Figure 4.25. are presented the reaction force curves (platforms number 1, 3 and 5 associated with the right leg and platforms number 2, 4 and 6 associated with the left foot) for the subject 3 during the test 3. Related curves were obtained for the 3 tests for all subjects.

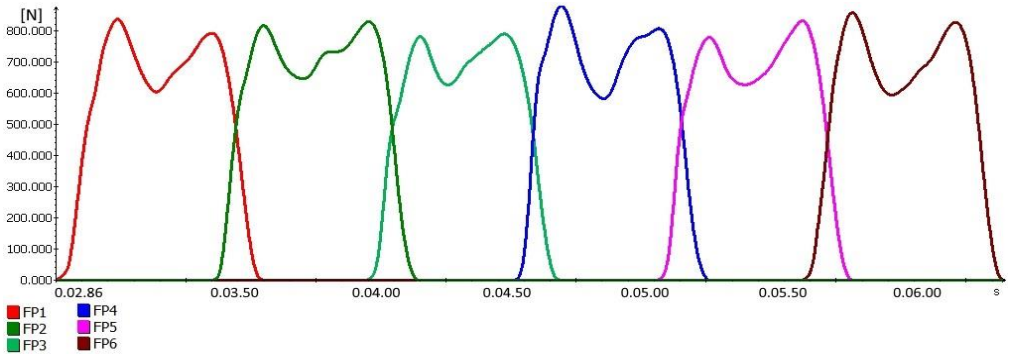

Fig. 4.25. Reaction forces diagram for the force platforms for subject 3 and T3 test

As in the case of flexion-extension angles, and for reaction forces, mean cycles and standard deviations (+ StdDev and -StdDev) were determined in the form of diagrams. The mean cycle of the reaction forces obtained in the sample of 14 healthy subjects on the 6 force platforms corresponding to Test 1 are shown in Figure 4.26.

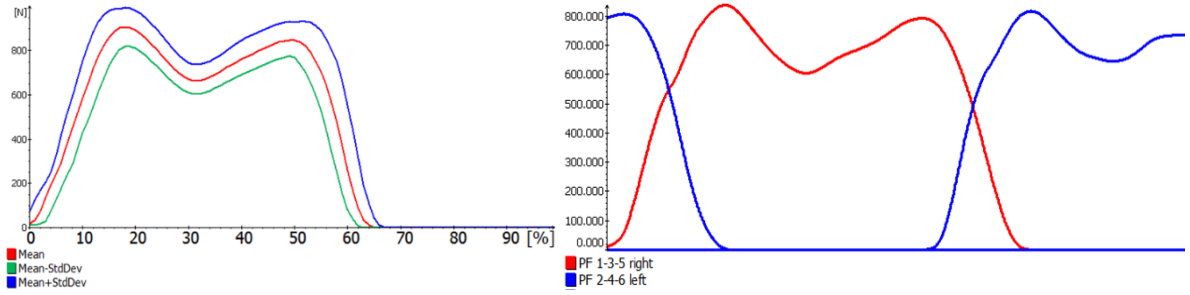

a) b)

Fig. 4.26 a) Mean cycle, Mean cycle + StdDev and Mean cycle - StdDev of reaction forces determined experimentally for right leg, T3 test; b) Mean cycles of the experimental reaction forces for the right leg and the left leg 1 - Test 1

4.6. Patient results

In figures 4.29. the diagrams of the results obtained after the T1, T2 and T3 tests by the patients are presented. Similar charts were obtained for the other tests.

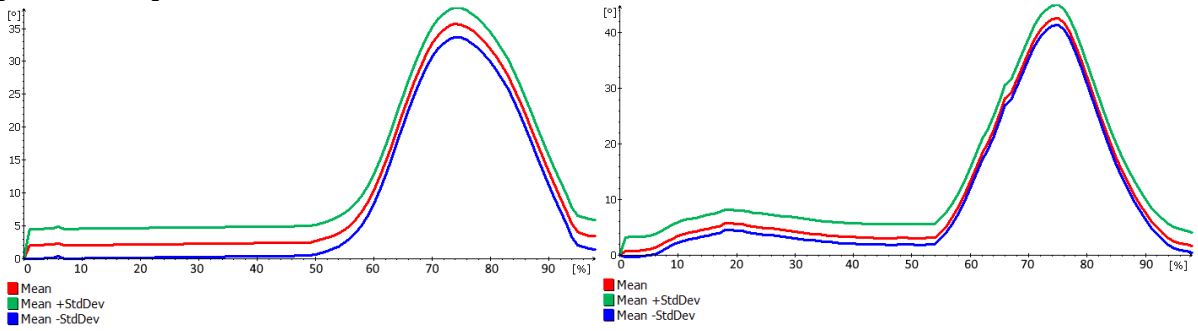

a) b)

Fig. 4.29. Diagram of the mean cycle, mean cycle + StdDev and mean cycle - StdDev: a) T1 test - righ knee - sample patients; b) T1 test - right knee - sample patients after surgery

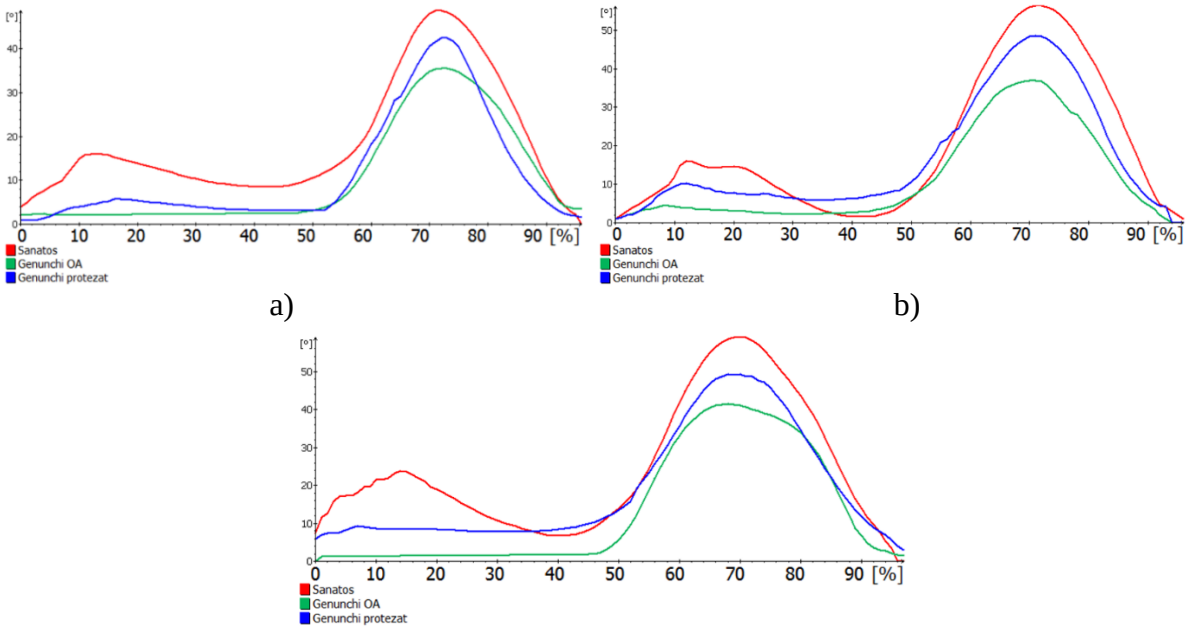

Fig. 4.32. Diagram of comparison of the mean cycle of the sample of healthy subjects, sample patients before surgery and sample patients after surgery for a) test T1; b) test T2 and c) test T3.

4.7. Own contributions

1. Manage the entire data acquisition process.
2. Acquiring a total of 2,472 experimental data files, processing files, and obtaining mean cycle diagrams of flexion-extension angles for the 6 lower limb joints of each healthy subject and patient, and obtaining diagrams for mean cycle at sample level.
3. Processing the data collected for the reaction forces and obtaining their mean cycles corresponding to the 3 experimental ground walking tests for both healthy subjects and patients.

Chapter 5. Mathematical modelling of walking

5.1. Introduction

The objective of this chapter is to develop an analytical model of the human movement on the ground in order to determine numerically the grinding forces with the ground during the walk.

In order to achieve this goal, it starts from the idea that the human organism is modeled as being made up of several bodies connected to each other, each body attaching to its own reference system.

Several kinematic chains can be highlighted:

- Two kinematic chains corresponding to the two lower limbs;
- Two kinematic chains generated by the upper limbs.

In developing the mathematical model of the human walking movement, we are particularly interested in the two kinematic chains of the lower limbs, so they will be shown in the basic scheme associated with the human body. Figure 5.1 shows the kinematic chains of the human lower limbs and the axle systems attached to the human body model..

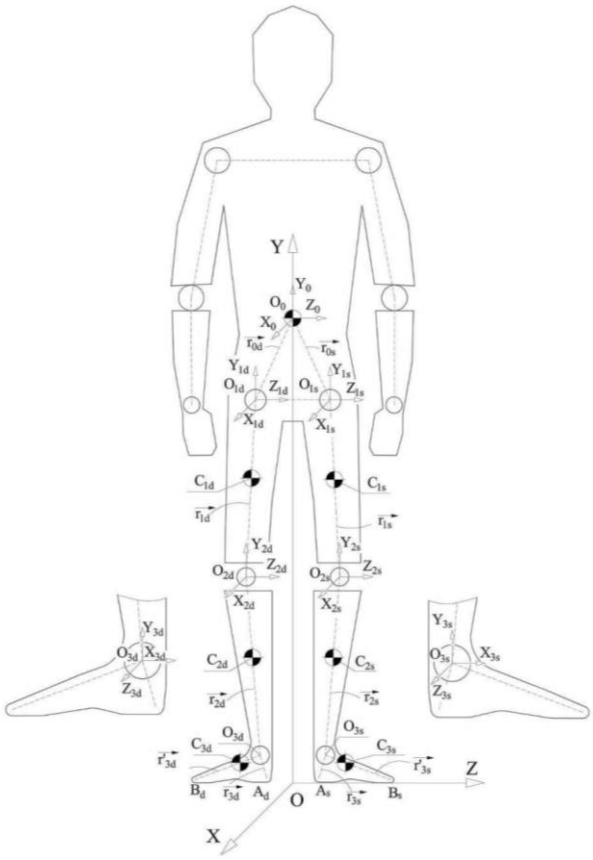

Fig. 5.1. Kinematic chains of human lower limbs and attached axle systems

5.2. Defining the kinematic matrices of the origins of the attached axle systems

We note with O_0, the origin of the reference system attached to the trunk of the human body, namely, $X_OO_OY_OZ_O$. Matrix of point coordinates O_0 compared to the outer mark is (R_0).

In addition to reference systems attached to component parts, the whole assembly is reported to an outside reference system considered as fixed, XOYZ.

The connection between the body 1_s of the left lower limb (symbolized by s) and body B is considered to be in the point O_1, which is the origin of the reference system attached to the body 1_s, namely, $X_{1s}\,O_{1s}\,Y_{1s}\,Z_{1s}$.

Matrix of point coordinates O_{1S} compared to the outer mark is:

$$(R_{1s}) = (R_0) + [S_0](r_{0s}) \quad (1)$$

- where:

$[S_0]$ is the coordinate change matrix from the mark attached to the body B at the outer marker;

(r_{os}) is the point coordinate matrix O_{1s} relative to the body marker B.

The connection between the body 1_S and body 2_S it is considered to be at the point O_{2S}, which is the origin of the reference system attached to the body $2_{S,}$ namely, $X_{2s}\,O_{2s}\,Y_{2s}\,Z_{2s}$.

Similarly defines matrices (R_{2s}) and (R_{3s}))

Matrix of point coordinates O_o compared to the outer mark is:

$$(V_0) = (\dot{R}_0) \quad (6)$$

Matrix of the acceleration of the point O_0 is:

$$(a_0) = (\dot{V}_0) = (\ddot{R}_0) \quad (7)$$

Matrix of the velocity of the point O_{1S} compared to the outer mark is:

$$(V_{1s}) = (V_o) + [\omega_o][S_o](r_{os}) \quad (8)$$

In which $[\omega_o]$ is the matrix of the angular velocity of the body B.

Matrix of the acceleration of the point O_{1S} compared to the outer mark is:

$$(a_{1s}) = (a_o) + [\varepsilon_o][s_o](r_{os}) + [\omega_o]^2[s_o](r_{os}) \quad (9)$$

with

$$[\omega_o]=[\dot{s_o}][s_o]^t \quad (10)$$

In which $[\varepsilon_o]= [\dot{\omega_o}]$ is the matrix of the angular acceleration of the body B.

Similarly, similar relationships are written for the other origins of the attached reference systems

5.4. Determination of kinetic matrices of joints and mass centres of the kinematic chain of the lower limb

In Figure 5.2. are presented. the schematic diagram defining the experimental angles (as defined in the Biometrics system) and the theoretical angles used in the development of the mathematical model of walking.

The link formulas between the theoretical and experimental angles collected by the Biometrics biomechanical data acquisition system are:

$$\varphi_1 = 270° + \varphi_h \quad (38)$$

$$\varphi_2 = \varphi_1 - \varphi_k \quad (39)$$

$$\varphi_3 = \varphi_2 + 90° + \varphi_a \quad (40)$$

$$\varphi_a = \varphi_a' + \varphi_a'' \quad (41)$$

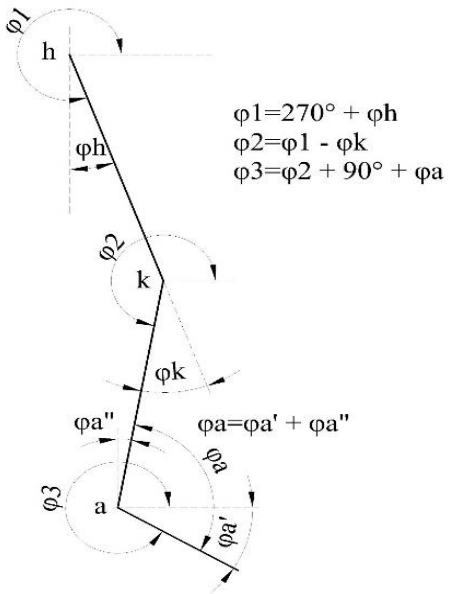

Fig. 5.2. The experimental and theoretical angles of the lower limb joints

5.5. Determination of analytical expressions of ground reaction forces

Load the system with forces and inertia couples. If plane motion is considered to be, inertial forces and couples will be:
- For the trunk:

$$\vec{F}_{in,o} = -m_o a_{ox}\vec{\imath} - m_o a_{oy}\vec{J} \quad (74)$$

$$\vec{M}_{in,o} = -J_o \ddot{\varphi}_o \vec{k} = 0 \quad (75)$$

- For the kinematic chain "s":

$$\vec{F}_{in,is} = -m_{is} a_{cisx}\vec{\imath} - m_{1s} a_{cisy}\vec{J} \quad (76)$$

$$\vec{M}_{in,1s} = -J_{is}\ddot{\varphi}_{is}\vec{k} \quad (77)$$

The motion equations are:

$$\begin{cases} T_s + T_d = T \\ N_s + N_d = N \\ X_A N_s + X_B N_d = M \end{cases} \quad (84)$$

where:

$$T = m_o a_{ox} + \sum_{i=1}^{3} m_{is} a_{cisx} + \sum_{i=1}^{3} m_{id} a_{cidx} \quad (85)$$

$$N = m_o a_{oy} + \sum_{i=1}^{3} m_{is} a_{cisy} + \sum_{i=1}^{3} m_{id} a_{cidy} + (m_o + \sum_{i=1}^{3} m_{is} + \sum_{i=1}^{3} m_{id}) * g \quad (86)$$

$$M = m_o\left(X_o a_{oy} + X_o g - Y_o a_{ox}\right) + \sum_{i=1}^{3} m_{is}(X_{is} a_{cisy} + X_{is} * g - Y_{is} a_{cisx}) + \sum_{i=1}^{3} m_{id}(X_{id} a_{cidy} + X_{id} * g - Y_{id} a_{cidx}) + \sum_{i=1}^{3} J_{is}\,\ddot{\varphi}_{is} + \sum_{i=1}^{3} J_{id}\,\ddot{\varphi}_{id} \quad (87)$$

Reacțiunile normale pe sol sunt date de formulele:

$$N_s = \frac{M - N * X_B}{X_A - X_B} \quad (88)$$

$$N_d = \frac{N * X_A - M}{X_A - X_B} \quad (89)$$

5.6. Numerical results

Following each step of the calculation algorithm and applying the relationships defined in paragraph 5.4, a series of discrete values and a diagram of the reaction force with the ground corresponding to a running cycle are obtained.

In Figure 5.5. are presented the comparative graph of the ground reaction force resulting from the average cycle mathematical model and the average cycle plot at the sample level of the reaction force obtained experimentally.

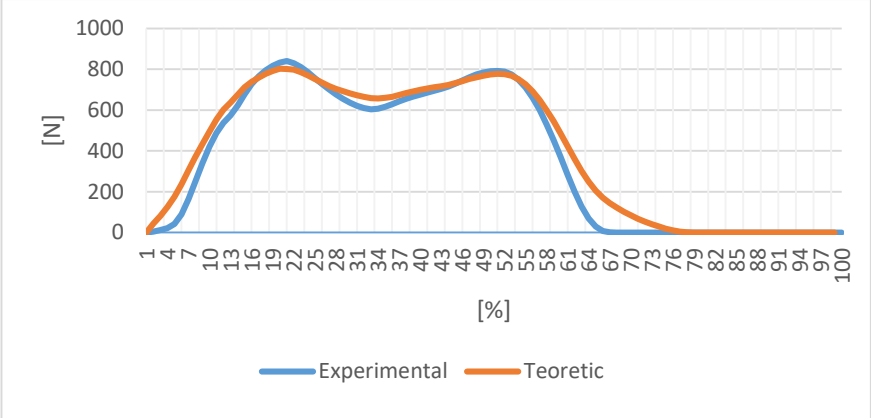

Fig. 5.5. Comparison of the experimental and theoretical diagram of the variation of the reaction forces with the ground

Own contributions

Elaboration of the mathematical model of the normal speed walking on the ground in order to finally obtain the calculation expressions of the variation of the ground reaction forces during a walking cycle.

Chapter 6. Virtual modeling of the proposed exoskeleton for rehabilitation of walking

6.1. Introduction

The development of the new device has started from the idea of reproducing the movement of the lower limbs as close as possible to the human one and the possibility of varying the flexion-extension angles for each joint.

Conception of the device began with the study of components of the bone system of the lower limbs, thus taking into account the position of the components of the bone system, their dimensions and the movements performed by the lower limbs. The development started with the sketches for each component followed by the construction of the parts so that the system finally passed a series of tests to validate it according to the literature.

A second step in developing the device is to collaborate with specialist physicians to find a solution that meets the needs of patients who have suffered an accident or who have undergone lower limb surgery. Discussions have resulted in a number of ideas that have been implemented in the recovery device.

The proposed exoskeleton aims to recover and improve walking in people with lower limb disorders. Diseases can be both in the knee joint, this being the most common case, but also in the hip or ankle joints. Therefore, the proposed device can adapt to a recovery of the joint motion of both lower limbs or only a lower member.

.

6.2. The virtual model

The virtual model is shown in Figure 6.1.a. The solution presented is one with low energy consumption, for the actuation of the whole device, a single rotary motor is used which drives by means of chain transmission the element 1 which is fixed to the frame. The device features 8 elements and 10 rotation spindles in its structure.

6.2.1. The metal frame is designed to meet a number of features: Simple construction; Modularity; Enhanced ergonomics; Safety.

In Figure 6.1.b. the virtual model of the metal support frame for the exoskeleton arms is presented.

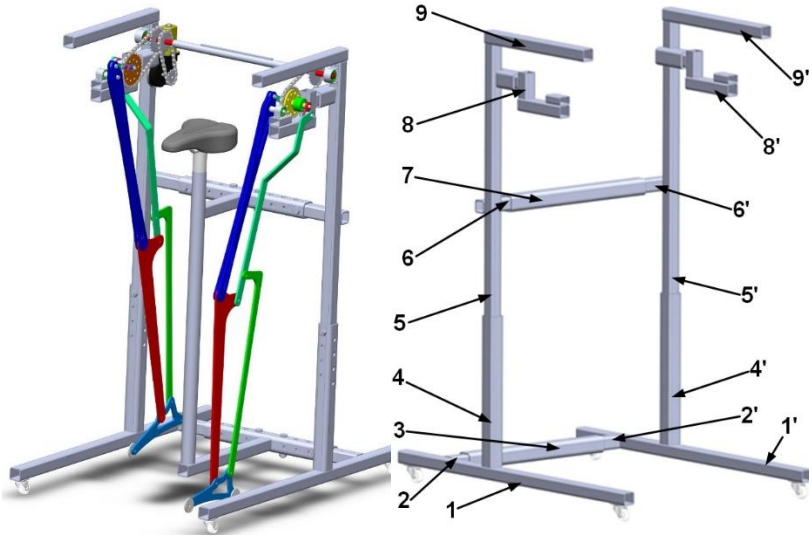

a) b)

Fig. 6.1. a) The virtual model of the exoskeleton b) The virtual model of the metal frame

6.2.2. The lower limbs of the exoskeleton

The exoskeleton was thought and designed in a similar way to the human lower limbs, both in terms of the mechanical model and the drive system, as well as in terms of size, shape and overall appearance. The dimensional and mass characteristics of the lower limbs have been studied for the purpose of imposing them as input data in the design of the exoskeleton. The virtual model of the inferior limb of the exoskeleton is shown in Figure 6.2.

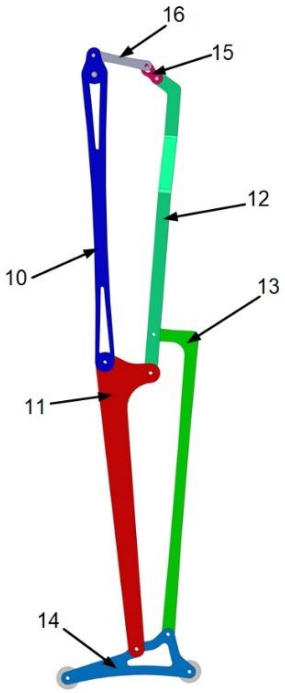

Fig. 6.2. The virtual model of the inferior limb of the exoskeleton

In Figure 6.3. is presented the subassembly corresponding to the right inferior limb of the exoskeleton - sagital plan view, as well as the kinematic scheme. The elements in Figure 6.3. b) have the following meanings:

- Item 10 - bar type element corresponding to the femur;
- Item 11 - bar type element corresponding to the tibia;
- Item 12 - bar type element that helps to achieve the flexion-extension angle of the knee;
- Item 13 - bar type element that helps to achieve the flexion-extension angle of the ankle;
- Item 14 - bar type element for the foot;
- Item 15 and 16 - bar type elements by which the amplitude of the flexion-extension angle of the three joints is adjusted;
- Item 17 - a chain toothed wheel that converts the rotation motion of the electric motor into a pivotal motion of the elements 10 and 13;
- Items 18, 19 and 20 - chain gears that are part of the power transmission system;
- Items 21 and 22 - chains through which power is transmitted;
- Item 23 - Electric engine

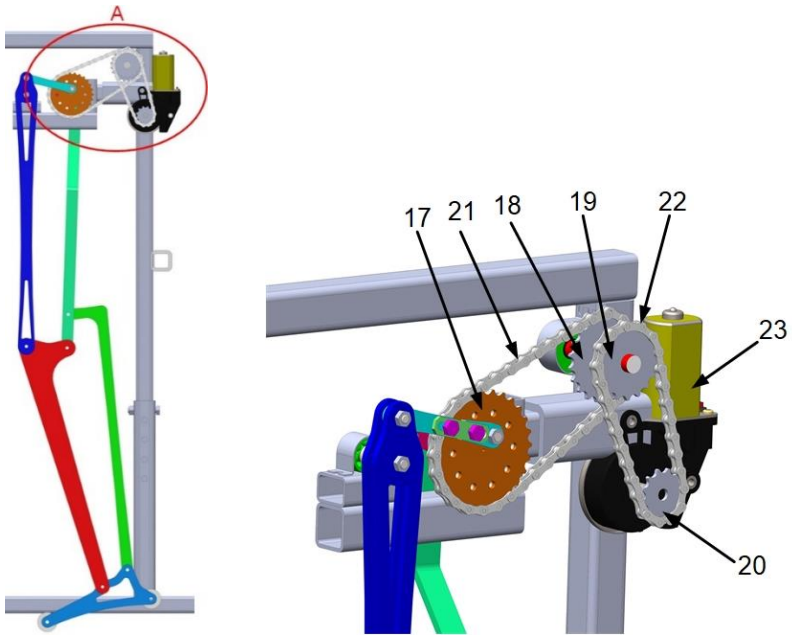

a) c)

Fig. 6.3. a) Part corresponding to the right lower limb of the exoskeleton - sagittal plane view (the numbering of the elements is shown in Figure 6.2); c) detail A - power transmission system

The entire movement of the exoskeleton is generated by a single electric motor. The transmission of power from the engine to the two lower limbs of the exoskeleton is achieved by mechanical transmission with toothed wheels (Figure 6.3, Positions 18, 19 and 20) and chains (Figure 6.3, Items 21 and 22).

6.2.3. The movement of the exoskeleton hip joint, is inspired by human hip movement, the device being designed to provide a flexion-extension movement that meets the experimentally measured parameters on subjects. The main component of the hip joint is the element 10 similar to the human femur

In Figure 6.4. the virtual model of the hip joint of the exoskeleton is presented.

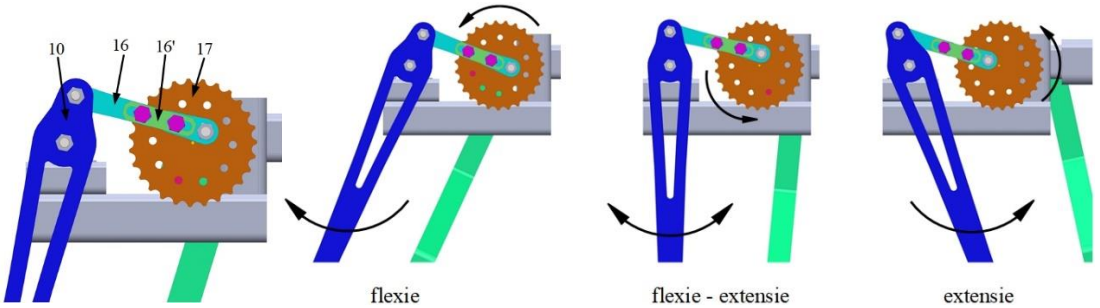

Fig. 6.4. The virtual model of the exoskeleton hip joint Fig. 6.5. The principle of hip joint functioning.

6.2.4. The movement of the exoskeleton knee joint is inspired by the movement of the human knee. The mechanism is designed to perform a flexion-extension movement that meets experimentally measured parameters on subjects. The knee joint is composed of two main elements (Figure 6.6. a) items 10 and 11) and a secondary element (Figure 6.6.b) item 12).

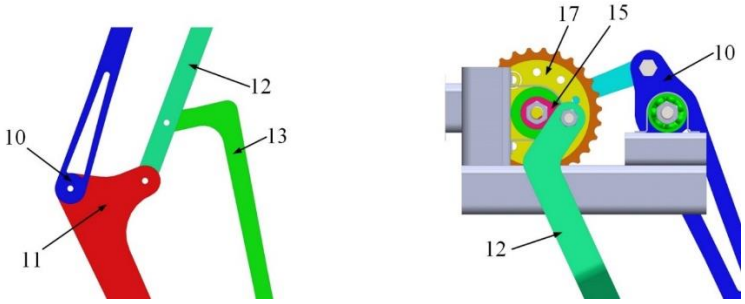

a) b)

Fig. 6.6. a) Virtual knee joint model; b) Movement system to the knee joint

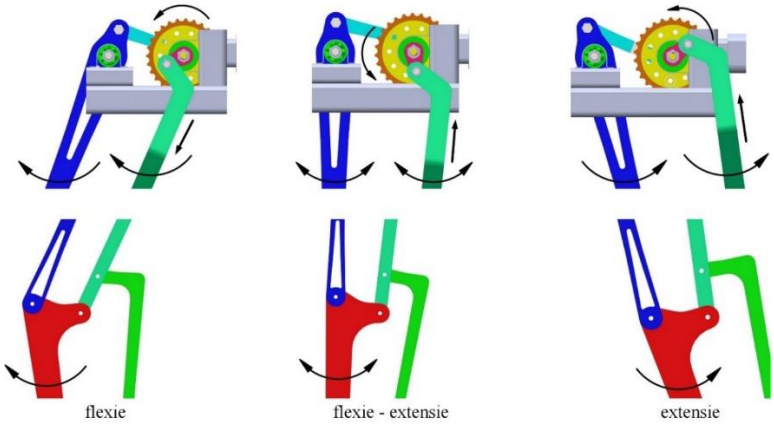

Fig. 6.7. The principle of knee joint operation..

6.2.5. The movement of the exoskeleton ankle joint is the result of the action of two main elements: the element 11 representing the tibia and the element 14 representing the foot, as well as a secondary element (Figure 6.8, Item 13). The movement of the ankle joint, unlike the other two joints, is not driven by the electric motor, but is the result of the combination of the movements of the three elements mentioned above (Figure 6.8, Item 11, 13, 14). The flexion-extension angle of the ankle joint is formed by the movement of the knee joint to which the movement of the element 13 is added.

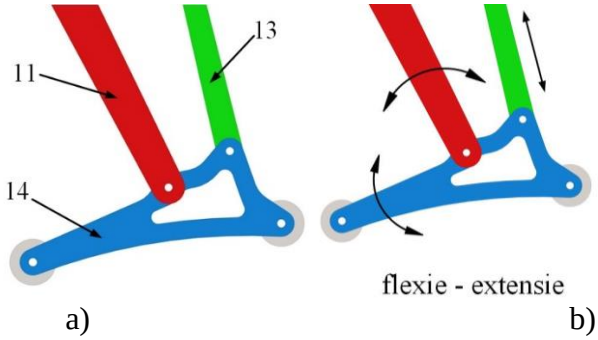

Fig. 6.8. a) Virtual ankle joint model b) Ankle joint operation principle
Kinematic analysis of the mechanism

6.3. The kinematic analysis

In Figure 6.9. the kinematic scheme of the mechanism is presented.

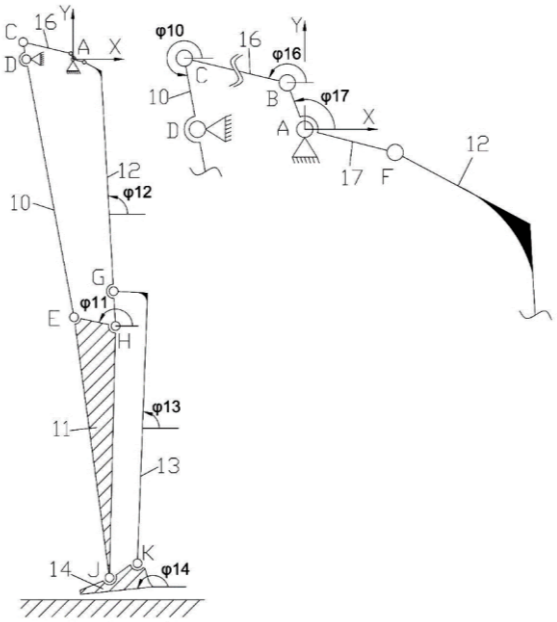

Fig. 6.9. The kinematic scheme of the mechanism

The calculation of the degree of mobility is done with the relation:

$$M = 3n - 2C_5 - C_4 = 3 * 7 - 2 * 10 = 1 \quad (6.1.)$$

They know each other:

-lenght of the elements:

lAB=11 mm, lBC=91mm, lCD=36mm, lCE=480mm, lAF=20mm, lFH=461mm, lGH=61mm, lGK= 465mm, lEJ=451mm, lEJ=451mm.

-coordinates of rotation couples connected to the base: xD=80mm, yD=0mm; YA=xA=0. The distance from the ground A coupling is 1050mm.

- the movement element of the leading element: $\omega_1 = 3rad/s$

The mechanism presents in the structure three RRR types: BCD, EHF, JGK

BCD

Ecuațiile pozițiilor:

$$\begin{cases} X_C = X_B + l_{BC} \cdot \cos\varphi_{16} = X_D + l_{CD} \cdot \cos\varphi_{10} \\ Y_C = Y_B + l_{BC} \cdot \sin\varphi_{16} = Y_D + l_{CD} \cdot \sin\varphi_{10} \end{cases} \quad (6.5.)$$

$$\begin{cases} (X_D - X_B) + l_{CD}\cos\varphi_{10} = l_{BC}\cos\varphi_{16} \\ (Y_D - Y_B) + l_{CD}\sin\varphi_{10} = l_{BC}\sin\varphi_{16} \end{cases} \quad (6.6.)$$

FHE

Ecuațiile pozițiilor:

$$\begin{cases} x_H = x_F + l_{FF'} \cdot \cos(\varphi_{12} + \pi - \beta) + l_{F'H} \cdot \cos\varphi_{12} = x_E + l_{EH} \cdot \cos\varphi_{11} \\ y_H = y_F + l_{FF'} \cdot \sin(\varphi_{12} + \pi - \beta) + l_{F'H} \cdot \sin\varphi_{12} = y_E + l_{EH} \cdot \sin\varphi_{11} \end{cases} \quad (6.18.)$$

Unde $\beta=121^o$

JKG

Ecuațiile pozițiilor

$$\begin{cases} x_K = x_G + l_{GG'} \cdot \cos(\varphi_{13} - \pi/2) + l_{G'K} \cdot \cos\varphi_{13} = x_J + l_{JK} \cdot \cos\varphi_{14} \\ y_K = y_G + l_{GG'} \cdot \sin(\varphi_{13} - \pi/2) + l_{G'K} \cdot \sin\varphi_{13} = y_J + l_{JK} \cdot \sin\varphi_{14} \end{cases} \quad (6.23.)$$

Positions, speeds and accelerations were calculated using Maple software.

Finally, a comparative diagram is presented between the normalized average of the flexion-extension angle of the osteoarthritic knee and the normalized cycle of the flexion-extension angle of the exoskeleton's knee.

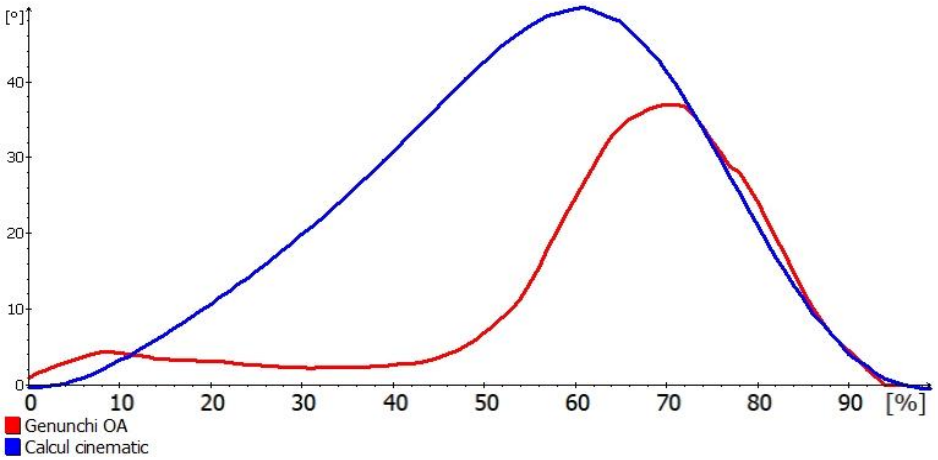

Fig. 6.10. Comparative graph - osteoarthritic knee and kinematic computation

From Figure 6.10. it is noted that the extensions of the exoskeleton's knee extensions are 12-15° greater than the OA knee and that in the first 50 percent of the cycle, the exoskeleton performs a movement similar to that of the healthy knee, with much amplitude higher than the knee OA. Similar charts were obtained for hip and ankle extension flexion angles.

These observations confirm the validity and accuracy of the virtual and physical prototype of the proposed exoskeleton in the thesis.

6.4. Realization of the physical prototype of the exoskeleton

An important step in the elaboration of the thesis was the realization of the physical prototype of the exoskeleton. The prototype was accomplished in several stages, starting from making the metal frame followed by making the elements of the lower limbs and the gears and finally assembling them on the metal frame.

In Figure 6.11. is presented the physical prototype of the exoskeleton where the metal frame is observed.

Fig. 6.11. The physical prototype of the exoskeleton.

6.5. Biomechanical evaluations of the exoskeleton

Using the Biometrics equipment described in Chapter 4, information was obtained on the exoskeleton's walking characteristics. For all 6 joints, variation diagrams of the flexion-extension angle were obtained, results that were compared with the results obtained in healthy subjects. The purpose of this study was to validate the feasibility of the device in a process of recovering the movements of the joints while walking. In figure 6.16. the data acquisition system mounted on the exoskeleton is presented.

Fig. 6.16. Biometrics equipment mounted on the exoskeleton

In figure 6.17. there is a diagram showing the variation of the extension flexion angles for the hip, knee and ankle joint.

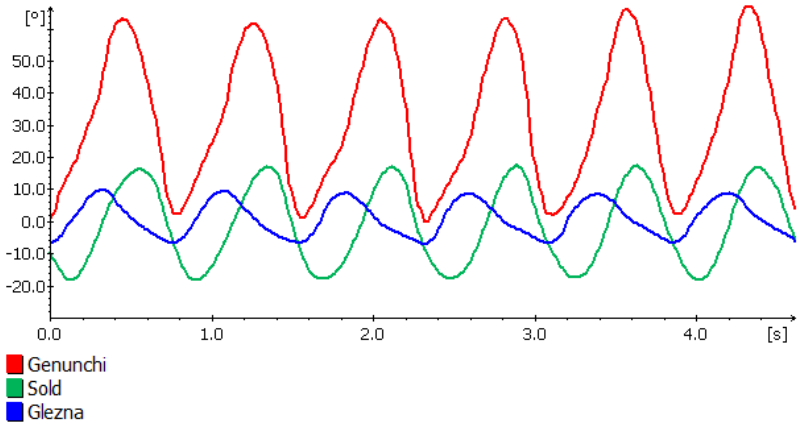

Fig. 6.17. Variation of extension angles of the hip, knee and ankle joint of the exoskeleton

The experimental data was processed using the method described in Chapter 4. The mean cycle diagrams for each joint were obtained. In figures 6.18.-6.20. the diagrams obtained from the exoschelet tests are presented.

In figures 6.21-6.23. comparative diagrams of the average hip, knee and ankle joints for the exoskeleton and for the healthy subject are presented.

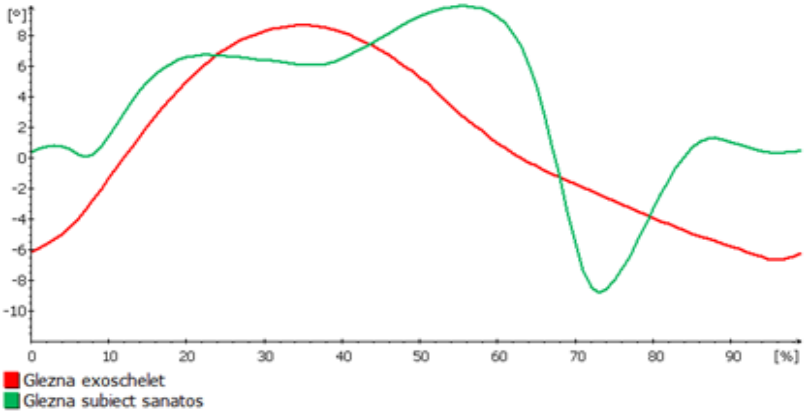

Fig. 6.21. Comparison of flexion-extension angle variation for ankle joint - exoskeleton and healthy subject

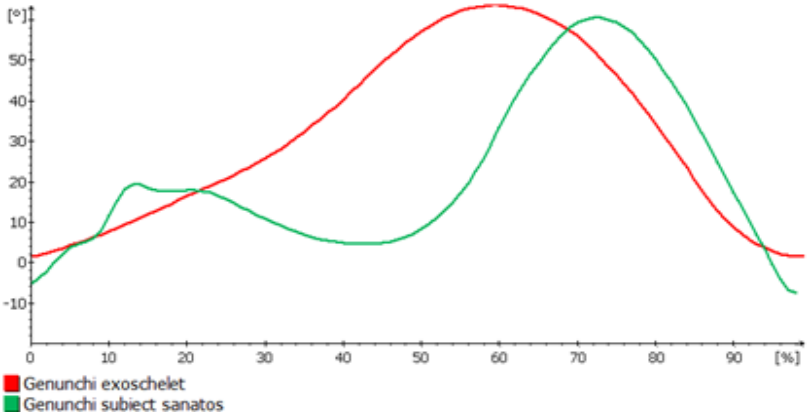

Fig. 6.22. Comparison of flexion-extension angle variation for knee joint - exoskeleton and healthy subject

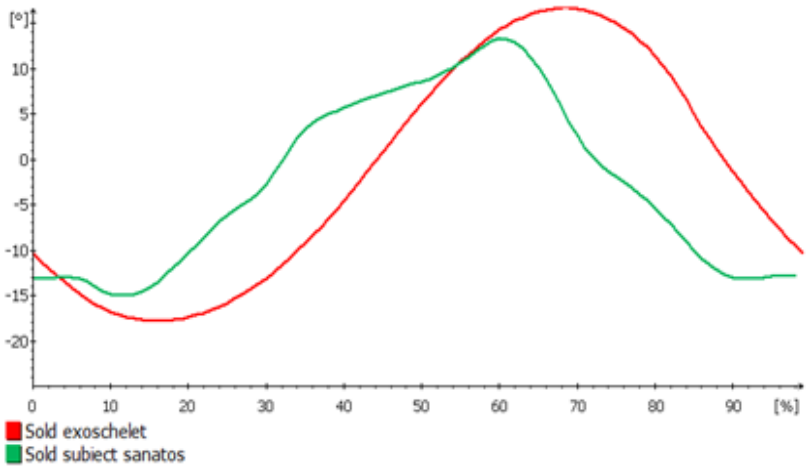

Fig. 6.23. Comparison of flexion-extension angle variation for hip joint - exoskeleton and healthy subject

Own contributions

- Developing the virtual model of the lower limb joint rehabilitation device.
- Execution of the physical prototype of the lower limb recovery device.
- Acquisition and processing of experimental data collected from the 6 joints of the rehabilitation device

Chapter 7. Simulating the Walking of a Virtual Mannequin Using the Adams Program

7.1. Introduction

In this chapter are presented the research in the direction of cinema and dynamics of human walking using the ADAMS software system [MSC2013]. Studies are focused on walking on the ground as well as walking on the treadmill.

7.2. Building the multibody model of the virtual mannequin

The virtual model of the mannequin developed and used in this chapter respects the kinematic structure and mass properties of the locomotor system. For ground contact, both sliding and impact with the ground, using the contact model by defining an impact function, are taken into account.

7.2.1. Definition of the kinematic model of the mannequin and the mass properties

In Figure 7.1. is presented the virtual assembly of the mannequin resulting from the assembly of the 13 parts, connected to each other by the kinematic couplers. The virtual model of the mannequin was developed and used in articles published by the author of the thesis together with the team with whom he collaborated during the research in the doctoral thesis [TAR2016/1, TAR2018/1, TAR2016/2].

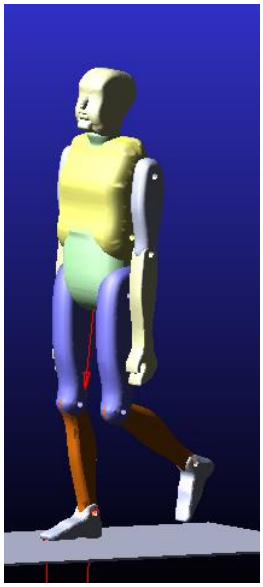

Fig. 7.1. Virtual model and simplified kinematic scheme of kinematic chains of human lower limbs

7.3. Results of simulation of walking on ground of the mannequin

The results obtained by the ADAMS simulation consist of graphical results representing the trajectories of the joints as well as numerical results. Vertical reaction forces developed in the joint of the hip, knee, ankle; the ground response forces of the mannequin are shown in figures 7.14.-7.17

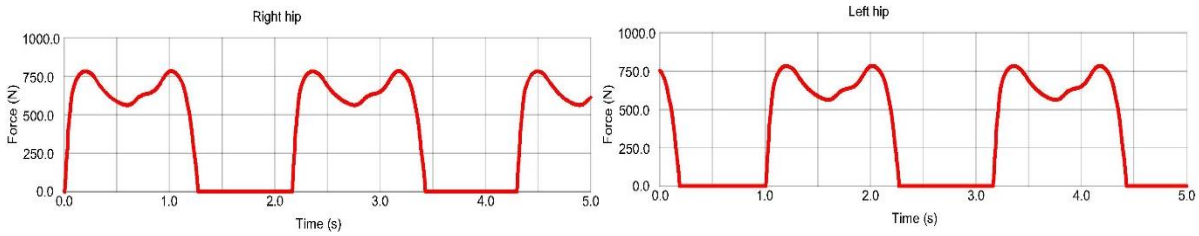

a) b)

Fig. 7.14. Variation of the reaction force for the articulation of the mannequin a) right hip b) left hip

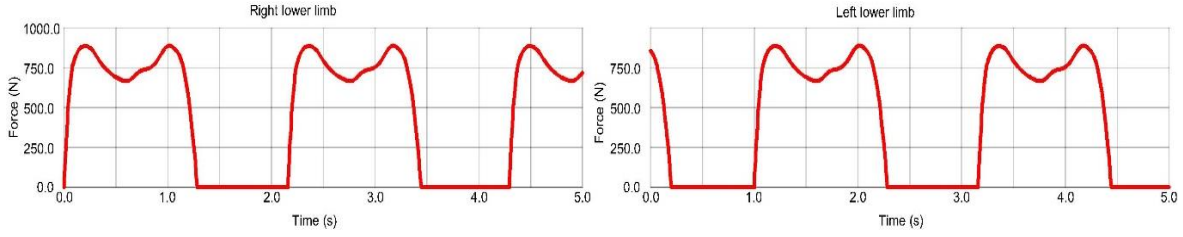

a) b)

Fig. 7.17. Variation of the ground response force for the lower limb of the mannequin a) right b) left

7.4. Results of the ground-walking simulation of the manniquin-exoschelet assembly

In this subchapter, we have proposed the modeling and simulation of the virtual exoskeleton assembly shown in figure 7.18, in the assumption of walking on the flat surface

(ground), having as starting point the experimental data obtained and the average cycle determined at the sampling level healthy subjects.

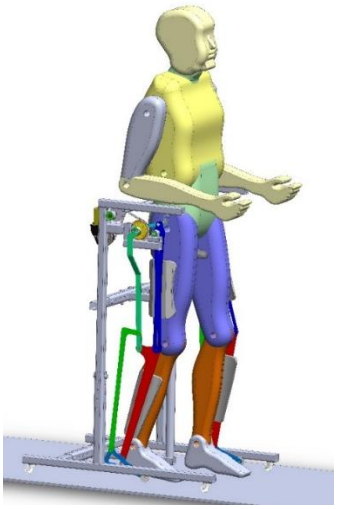

Fig. 7.18. The virtual mannequin - exoskeleton assemby on the ground

The numerical results for the walking simulation of exoskeleton attached on the mannequin are shown in figures 7.19.-7.21

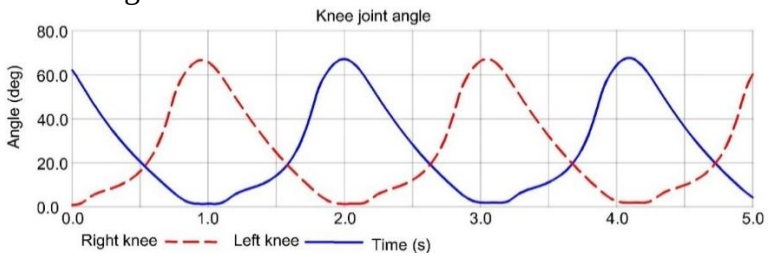

Fig. 7.19. Variation of flexion-extension angle of knee joints

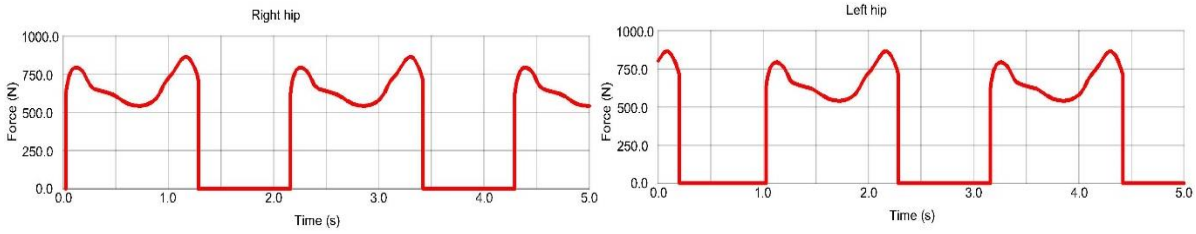

a) b)

Fig. 7.22. Variation of the hip joint reaction force: a) right hip b) left hip

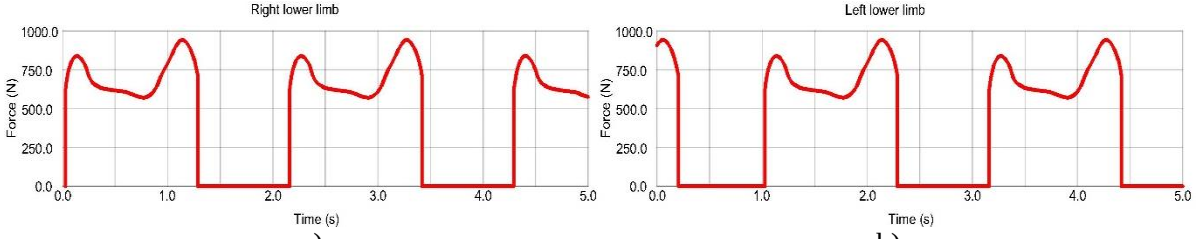

a) b)

Fig. 7.25. Variation of the reaction force with the ground for the left and right lower limbs

7.5. Results of walking on inclined treadmill simulation of the virtual mannequin - exoschelet assembly

For this simulation model, the exoskeleton is worn by the virtual human mannequin, the simulation model being complemented by a treadmill with the possibility of adjusting the

inclination. In Figure 7.28. the virtual model of the mannequin-exoskeleton assembly on the treadmill is presented.

Fig. 7.28. The virtual mannequin - exoskeleton assembly on the treadmill

The numerical results of walking simulation of exoskeleton on the mannequin are shown in Figures 7.29-7.32.

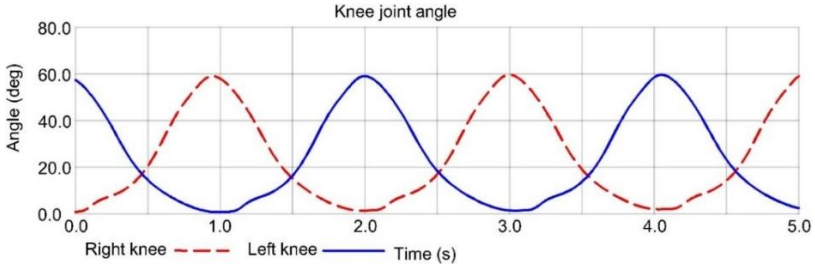

Fig. 7.29. Variation of flexion-extension angle of knee joint 2.5km/ h – 7°

Figures 7.33.-7.36. shows the reaction forces with the calculated contact surface for hip, knee and ankle joints of the exoskeleton to simulate walking on the treadmill at 2.5 km/ h and 3° and respectively 7°. Figure 7.36. shows the ground reaction forces of the exoskeleton for the right lower limb.

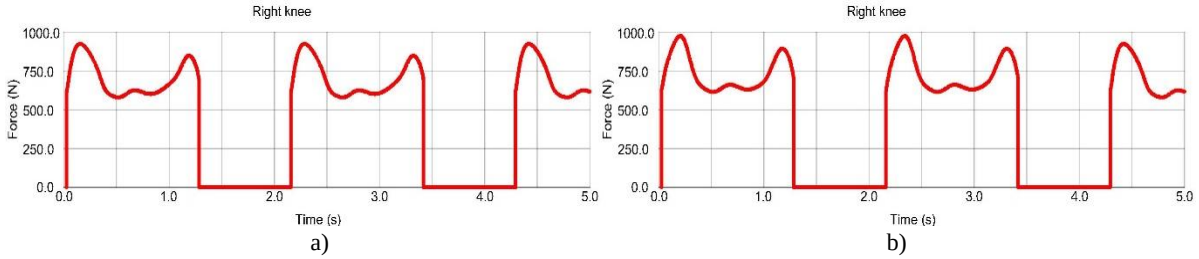

a) b)

Fig. 7.33. Variation of knee joint reaction forces for tests a) 2.5km/ h - 3° and b) 2.5km/ h – 7°

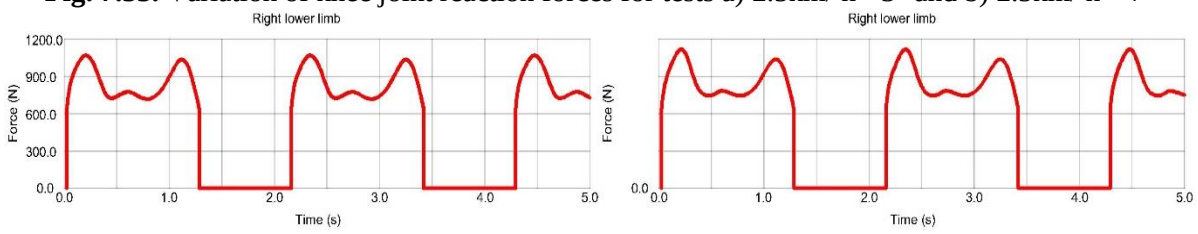

a) b)

Fig. 7.36. Variation of reaction forces in the lower right limb for the tests a) 2.5km/ h - 3° and b) 2.5km/ h – 7°

Own contributions

Simulation of mannequin walking in the ADAMS simulation environment in different phases: walking on the surface of the ground and on the treadmill, with and without exoskeleton.

Obtaining the charts and motion laws of the exoskeleton joints, as well as laws of time variation of the reaction forces with the ground and the reaction forces in the joints.

Chapter 8. Capitalizing on the Results, Original Contributions, and Future Research Directions

8.1. Capitalizing on the research results

The studies, analyzes and experimental results presented in this paper were disseminated through articles published in ISI Journals with impact factor, in the indexed volumes of international ISI or BDI conferences.

Articles published in ISI rated journals and ISI indexed volumes

1. Tarnita, D., Calafeteanu, D., Geonea, I., **Petcu Alin**, Tarnita, D.N., **Effects of malalignment angle on the contact stress of knee prosthesis components, using Finite element method**, Rom J Morphol Embryol, vol. 58(3), 2017. **(IF=0.67**)
   https://www.scopus.com/record/display.uri?eid=2-s2.0-85039735793&origin=inward&txGid=d58965006aafaafcd43f5b7f94814cb0
2. Tarnita, D., Geonea, I., **Petcu Alin**, **Experimental human walking and virtual simulation of rehabilitation on plane and inclined treadmill**, Springer Proceedings în Physics, vol. 198, pp. 149-155, 2018; (https://www.scopus.com/record/display.uri?eid=2-s2.0-85039436867&doi=10.1007%2f978-3-319-69823-6_18&origin=inward&txGid=3f93d7bc56ed0cf9d58209c5abecadd6)
3. Tarnita, D., Geonea, I., **Petcu Alin**, Tarnita, D.N., **Numerical simulations and experimental human gait analysis using wearable sensors**, Mechanisms and Machine Science, vol. 48, pp. 289-304, 2018.
   (https://www.scopus.com/record/display.uri?eid=2-s2.0-85028070019&doi=10.1007%2f978-3-319-59972-4_21&origin=inward&txGid=188814499f4949b5b92ae3662ff8680f)
4. Tarniţă, D., Geonea, I., **Petcu Alin**, Tarniţă, D.N., **Experimental characterization of human walking on stairs applied to humanoid dynamics**, Advances în Intelligent Systems and Computing, vol. 540, pp. 293-301, 2017.
   (https://www.scopus.com/record/display.uri?eid=2-s2.0-85007309854&doi=10.1007%2f978-3-319-49058-8_32&origin=inward&txGid=4fa2d055ddf4e91a0744d92a7b94cbae)
5. Tarnita, D., Georgescu, M., Geonea, I., **Petcu Alin**, Tarnita D.N., **Nonlinear analysis of human ankle dynamics**, Mechanisms and Machine Science, vol. 65, pp. 235-243. 2019.
   (https://www.scopus.com/record/display.uri?eid=2-s2.0-85054144495&doi=10.1007%2f978-3-030-00329-6_27&origin=inward&txGid=9f59343334f5fe2cf926f657c7e3e625)

Articles published in BDI volumes and magazines

6. Georgescu, M., **Petcu Alin**, Tarnita, D, **Influences of speed and treadmill inclination on the local dynamic stability of human knee joint**, Applied Mechanics and Materials, vol. 880, pp. 130-135, 2018; (https://www.scientific.net/AMM.880.130)
7. **Petcu Alin**, Georgescu, M., Tarnita, D., **Actuation systems of active orthoses used for gait rehabilitation**, Applied Mechanics and Materials, vol. 880, pp. 118-123, 2018. (https://www.scientific.net/AMM.880.118)

8. Geonea, I., Dumitru, N., Rosca, A.S., **Petcu Alin**, Ciurezu, L., **Experimental Validation of an Exoskeleton for Motion Assistancen**, Applied Mechanics and Materials, vol. 880, pp. 111-117, 2018. (https://www.scientific.net/AMM.880.111)
9. Tarniţă, D., Marghitu, D., **Petcu Alin**, **Nonlinear dynamics of human knee joint during jumps**, 35th Danubia Adria Symposium on Advances în Experimental Mechanics, 2018, (https://www.scopus.com/record/display.uri?eid=2-s2.0-85058281886&origin=resultslist&sort=plf-f&src=s&sid=22c521144643a89ee98d62207c907cba&sot=autdocs&sdt=autdocs&sl=18&s=AU-ID%2814051138200%29&relpos=6&citeCnt=0&searchTerm=)
10. **Petcu Alin**, Tarniţă, D., Geonea, I., Malciu, R., **Evaluation of human knee flexion-extension on inclined treadmill using wearable sensors**, 35th Danubia Adria Symposium on Advances în Experimental Mechanics, pp. 109-110, 2018. (https://www.scopus.com/record/display.uri?eid=2-s2.0-85058337454&origin=resultslist&sort=plf-f&src=s&sid=8c6bb388ab72a9ff7b77789884a9bb61&sot=autdocs&sdt=autdocs&sl=18&s=AU-ID%2842061278800%29&relpos=8&citeCnt=0&searchTerm=)
11. **Petcu Alin,** Calafetenu, D., Tarnita, D.N., **Numerical simulations and experimental flexion-extension measurements of human leg joints during squat exercises**, Medicina sportiva - Journal of the Romanian Sports Medicine Society, vol. XIII(1), pp. 2805-2811, 2017. (http://www.medicinasportiva.ro/SRoMS/RMS/47/simulations-experimental-flexion-extension-measurements-leg-joint-squat-exercises.pdf)
12. **Petcu, Alin,** Calafeteanu, D.**,** Georgescu, M., Tarnita, D., **Kinematics and kinetics of healthy and osteoarthric knee during walking stairs**. Bulletin of the Transilvania Univ. of Brasov, vol. 9(58), pp 203-208, 2016.
    (http://webbut.unitbv.ro/bulletin/Series%20I/BUT_PRASIC/Petcu%20A.pdf)
13. Georgescu, M., **Petcu Alin**, Tarnita, D., **Nonlinear movement of human knee overground & on treadmill**, Bulletin of the Transilvania University of Braşov, vol. 9(58) no. 2 - Special Issue Series I: Engineering Sciences, pp. 125-132, 2016.
    (http://rs.unitbv.ro/Bulletin/Series%20I/BUT_PRASIC/Georgescu%20M.pdf)

Participation in international conferences and congresses

- International Conference of Mechanical Engineering, **ICOME 2015,** Craiova, 2015
- The 25th International Conference on Robotics în Alpe-Adria-Danube Region, **RAAD 2016**, Belgrad 2016
- The IXth Product Design, Robotics, Advanced Mechanical & Mechatronic Systems and Innovation Conference, **PRASIC'16**, Braşov, 2016
- The 4th International Conference of Mechanical Engineering, **ICOME 2017,** Craiova, 2017
- European Exhibition of Creativity and Innovation, **EUROINVENT,** , Mai 2018

The Bronze Best Research Paper Award, awarded by The International Award Committee for MESROB2018 was obtained for the article:Tarnita D., Georgescu M., Geonea I., **Petcu Alin**, Tarnita D.N., **Nonlinear analysis of human ankle dynamics**, Mechanisms and Machine Science, Vol. 65, 2019, Pages 235-243, presented la International Symposium **New Trends in Medical and Social Robots, MESROB 2018, Cassino, Italy.**

Prizes and medals at the International Patent Salons for the patent application **"Device for the progressive recovery of the movements of the human joints used in orthotic systems", Inventors: Petcu Alin, Tarniţă Daniela, Tarniţă Dănuţ-Nicolae**, patent application no. A/00081, 2016

- **Diploma of excellence and gold medal with special mention** at the International Salon of Research, Innovation and Invention, **PROINVENT 2017, Cluj Napoca**

- **The cup and the special prize from the University „Lucian Blaga" Sibiu** at the International Salon of Research, Innovation and Invention, **PROINVENT 2017**
- **In Memoriam Ana Aslan** – at the The International Student Innovation and Scientific Research Exhibition - **"Cadet INOVA'17"**
- **Diploma of excellence and gold medal** at **EUROINVENT 2017**
- **Innovation Award from Polytechnic University of Bucharest** at the European Exhibition of Creativity and Innovation, **EUROINVENT 2017, Iasi.**
- **The diploma of Excellence and the Gold Medal from the Technical University of Moldova** an the European Exhibition of Creativity and Innovation, **EUROINVENT 2017, Iasi.**


The International Federation
for the Promotion of Mechanism and Machine Science

MESROB 2018
6-th International Workshop on New Trends in Medical and Service Robotics
4-6 July 2018: Cassino, Italy

The International Award Committee for MESROB 2018

presents
the Bronze Best Research Paper Award to
Daniela Tarnita, Marius Georgescu, Geonea Ionut Daniel, Alin Petcu, Danut-Nicolae Tarnita

In testimony of a significant achievement in Medical and Service Robotics with paper:
Nonlinear Analysis of Human Ankle Joint Dynamics

Cassino: July 5, 2018
Prof. Giuseppe Carbone, Chair of MESROB2018
Prof. M. Ceccarelli, Prof. A. Laribi, Prof. D. Pisla, the 2018 Award Committee


DIPLOMA
OF GOLD MEDAL Inventions Section is awarded to:
Device for recovering the progressive movements of human joints used in orthotic systems
Petcu Alin Ionel, Daniela Tarnita, Tarniță Dănuț Nicolae
EUROINVENT 2017


University POLITEHNICA of Bucharest
THE POLITEHNICA INNOVATION AWARD
DEVICE FOR RECOVERING THE PROGRESSIVE MOVEMENTS OF HUMAN JOINTS USED IN ORTHOTIC SYSTEMS
PETCU ALIN IONEL, DANIELA TARNIȚĂ, TARNIȚĂ DĂNUȚ NICOLAE
for achieving excellency in innovation through dedication and the consistent wish to push the borders of what can be obtained through science and technology


Republica Moldova Ministerul Educației
DIPLOMĂ DE EXCELENȚĂ
ȘI MEDALIA DE AUR
a Universității Tehnice a Moldovei,
se acordă
Drd.ing. Alin Petcu, prof.dr.ing. Daniela Tarniță, prof.dr. Dan Tarniță
pentru
DEVICE FOR RECOVERING MOVEMENTS OF HUMAN JOINTS USED IN ORTHOTIC SYSTEMS
Rector, dr.hab.prof.univ. Viorel Bostan
Secretar științific al Senatului Ion Sobor


"Lucian Blaga"
University of Sibiu
ROMANIA
awards
a Special Prize
as a sign of honor, recognition and appreciation
of scientific creativity and originality
to inventors
Alin Ionel Petcu, Daniela Tarniță, Dănuț Nicolae Tarniță

for invention
Dispozitiv pentru recuperarea progresivă a mișcărilor articulațiilor umane utilizat în sisteme ortopedice
Device for recovering the progressive movements of human joints used in orthopedic systems

Rector of "Lucian Blaga" University of Sibiu
Prof. Eng. Ioan BONDREA, Sc.D.

Manager of PatLib Sibiu Centre,
Prof. Eng. & Ec. Mihail Aurel ȚIȚU, Sc.D. & Ph.D.

Cluj-Napoca, 22nd - 24th March 2017
15th International Exhibition of Research, Innovation and Inventions PRO INVENT


The International Student Innovation and Scientific Research Exhibition
- "Cadet INOVA'17" -
The "Nicolae Bălcescu" Land Forces Academy of Sibiu, Romania
27-29 April 2017

THE "Cadet INOVA'17"
"IN MEMORIAM - GERONTOLOGIST INVENTOR, ACAD. PROF. ANA ASLAN, MD, PhD (1897 – 1988)" PLAQUETTE

Is bestowed on the researcher/researchers
Alin Ionel PETCU, Daniela TARNIȚĂ, Dănuț Nicolae TARNIȚĂ.

for the innovation:
DEVICE FOR RECOVERING THE PROGRESSIVE MOVEMENTS OF HUMAN JOINTS USED IN ORTHOTIC SYSTEMS

Member of the Jury,
MD
Ioan Gabriel BUCIUȚA PhD

President of the Exhibition,
Dipl. – Eng.
Silviu Mihai PETRIȘOR, PhD

SALONUL INTERNAȚIONAL AL CERCETĂRII, INOVĂRII ȘI INVENTICII
PRO INVENT
Ediția a XV-a, 2017, Cluj-Napoca, România
UNIVERSITATEA TEHNICĂ

DIPLOMA
DE EXCELENȚĂ
ȘI MEDALIA DE AUR CU MENȚIUNE SPECIALĂ

Se acordă: Alin Ionel Petcu, Daniela Tarniță, Dănuț Nicolae Tarniță
De la: Universitatea din Craiova
Pentru: Dispozitiv pentru recuperarea progresiva a miscarilor articulatiilor umane utilizat in sisteme ortotice

PREȘEDINTELE SALONULUI
Prof. dr. ing. VASILE TOPA
Rector al Universității Tehnice din Cluj-Napoca

PREȘEDINTELE JURIULUI
Prof. dr. ing. RADU MUNTEANU

Own contributions

1. Achieve a state-of-the-art synthesis of lower limb recovery systems as well as analysis methods and human lower limb joints.
2. Manage the entire data acquisition process.
3. Acquiring a total of 2,472 experimental data files, processing files, and obtaining mean cycle diagrams of flexion-extension angles for the 6 lower limb joints of each healthy subject and patient, and obtaining diagrams for mean cycle at sample level.
4. Processing the data collected for the reaction forces and obtaining their mean cycles corresponding to the 3 experimental ground walking tests for both healthy subjects and patients.
5. Elaboration of the mathematical model of the normal speed walking on the ground in order to finally obtain the calculation expressions of the variation of the ground reaction forces during a walking cycle.
6. Developing the virtual model of the lower limb joint rehabilitation device.
7. Execution of the physical prototype of the lower limb recovery device.
8. Acquisition and processing of experimental data collected from the 6 joints of the rehabilitation device
9. Simulation of mannequin walking in the ADAMS simulation environment in different phases: walking on the surface of the ground and on the treadmill, with and without exoskeleton.
10. Obtaining the charts and motion laws of the exoskeleton joints, as well as laws of time variation of the reaction forces with the ground and the reaction forces in the joints.

8.2. Future research directions

Future research directions address the following issues:

- Realization of the physical prototype of the device in the patent application;
- Development of an active knee orthosis;
- Patenting of the exoskeleton device for the knee and ankle joint rehabilitation proposed in the thesis

Patent Application - under evaluation

Device for the progressive recovery of the movements of the human joints used in orthotic systems, Inventors: Petcu Alin, Tarniţă Daniela, Tarniţă Dănuţ-Nicolae, patent application no. A/00081, 2016.

Bibliography

[PET2016] **Petcu Alin,** Calafeteanu, D., Georgescu, M., Tarnita, D., Kinematics and kinetics of healthy and osteoarthric knee during walking stairs. Bulletin of the Transilvania Univ. of Brasov, vol. 9(58), pp 203-208, 2016.

[PET2017] **Petcu Alin,** Calafetenu, D., Tarnita, D.N., Numerical simulations and experimental flexion-extension measurements of human leg joints during squat exercises, Medicina sportiva - Journal of the Romanian Sports Medicine Society, vol. XIII, no. (1), pp. 2805-2811, 2017.

[PET2018] **Petcu Alin**, Georgescu M., Tarnita D., Actuation systems of active orthoses used for gait rehabilitation, Applied Mechanics and Materials, vol. 880, pp. 118-123, 2018.

[PET2018/1] **Petcu Alin**, Tarniţă, D., Geonea, I., Malciu, R., Evaluation of human knee flexion-extension on inclined treadmill using wearable sensors, 35th Danubia Adria Symposium on Advances în Experimental Mechanics, pp. 109-110, 2018.

[TAR2013/a] Tarnita, D., Marghitu, D.B., Analysis of a hand arm system. Robot Comput Integr Manuf, vol. 29(6), pp. 493–501, 2013.

[TAR2013/b] Tarnita, D., Catana, M., Tarnita, D.N., Nonlinear analysis of normal human gait for different activities with application to bipedal locomotion, Rev Roum Sci Tech Mech Appl, vol. 58(1–2), pp. 177–188, 2013.

[TAR2013/c] Tarniţă, D., Catană, M., Tarniţă, D.N., Experimental measurement of flexion-extension movement in normal and osteoarthritic human knee, Rom J Morphol Embryol, vol. 54(2), pp. 309–313, 2013.

[TAR2014/a] Tarnita, D., Calafeteanu, D., Matei, I., Tarnita, D.N., Experimental measurement of flexion-extension in normal and osteoarthritic knee during sit-to-stand movement, Appl Mech Mater, vol. 658, pp. 520–525, 2014.

[TAR2016/1] Tarnita, D., Wearable sensors used for human gait analysis, Rom J Morphol Embryol, vol. 57(2), 309-313, 2016.

[TAR2016/2] Tarnita, D., Geonea, I., **Petcu Alin,** Tarnita, D.N., Experimental Characterization of Human Walking on Stairs Applied to Humanoid Dynamics, Advances in Robot Design and Intelligent Control, Advances in Intelligent Systems and Computing vol. 540, pp. 293-301, 2016.

[TAR2016/5] Tarnita D., Rosca A., Geonea I, Calafeteanu D., Experimental measurements of the human knee flexion angle during squat exercises, Applied Mechanics and Materials, vol. 823, pp. 113-118, 2016.

[TAR2016] Tarniţă, D.N., Tarniţă, D., Grecu, D., Calafeteanu, D., Căpităneşcu, B., New technical procedure involving Achilles tendon rupture treatment through transcutaneous suture, Rom J Morphol Embryol, vol. 57(1), pp. 211–214, 2016.

[TAR2017] Tarnita D., Calafeteanu D., Geonea I., **Petcu Alin**, Tarnita DN., Effects of malalignment angle on the contact stress of knee prosthesis components, using Finite element method, Rom J Morphol Embryol, vol. 58(3), 2017. (IF=0.67)

[TAR2018/1] Tarnita, D., Geonea, I., **Petcu Alin**, Experimental Human Walking and Virtual Simulation of Rehabilitation on Plane and Inclined Treadmill, Acoustics and Vibration of Mechanical Structures—AVMS-2017, Springer Proceedings in Physics vol. 198, pp. 149-155, 2018.

[TAR2018/2] Georgescu, M., **Petcu Alin,** Tarnita, D., Influences of speed and treadmill inclination on the local dynamic stability of human knee joint, Applied Mechanics and Materials, vol. 880, pp. 130-135, 2018.

[TAR2018/3] Tarniţă, D., Marghitu, D., **Petcu Alin**, Nonlinear dynamics of human knee joint during jumps, 35th Danubia Adria Symposium on Advances în Experimental Mechanics, 2018,

[TAR2019] Tarnita, D., Georgescu, M., Geonea, I., **Petcu Alin,** Tarnita, D.N., Nonlinear analysis of human ankle dynamics, Mechanisms and Machine Science, vol. 65, pp. 235-243. 2019.

[DT2016] Tarnita, D., Wearable sensors used for human gait analysis, Rom J Morphol Embriol, vol. 57(2), pp. 373-382, 2016.

[DTIG2018] Tarnita, D., Geonea, I., **Petcu, Alin,** Tarnita, D.N., Numerical Simulations and Experimental Human Gait Analysis Using Wearable Sensors, New Trends in Medical and Service Robots, Springer Publishing House, pp.289-304, 2018.

[DTMC2014] Tarnita, D., Catana, M., Tarnita, D.N., Contributions on the modeling and simulation of the human knee joint with applications to the robotic structures, New Trends on Medical and Service Robotics: Challenges and Solutions, Springer, pp. 283-297, 2014.

[DTMC2016] Tarnita, D., Catana, M., Tarnita, D.N., Design and Simulation of an Orthotic Device for Patients with Osteoarthritis, New Trends in Medical and Service Robots, Springer, pp 61-77, 2016.

[KS2014] Shamaei, K., et al, Design and functional evaluation of a quasi-passive compliant stance control knee–ankle–foot orthosis, vol. 22(2), pp. 258-268, 2014.

[KUN2011] Kun, L., Inoue, Y., Shibata, K., Enguo, C., Ambulatory estimation of knee-joint kinematics în anatomical coordinate system using accelerometers and magnetometers, IEEE Trans Biomed Eng, vol. 58, pp. 435–42, 2011.

[KUR2007] Kurtz, S., Ong, K., Lau, E., Mowat, F., Halpern, M., Projections of Primary and Revision Hip and Knee Arthroplasty în the United States from 2005 to 2030, J Bone Joint Surg Am, vol. 89(4), pp. 780 - 785, 2007.

[KY2002] Yamamoto, K., Hyodo, K., Ishii, M., Matsuo, T., Development of power assisting suit for assisting nurse labor, JSME International Journal. Series C, vol. 45(3), pp. 703-711, 2002.

[GEO2016] Georgescu, M., **Petcu Alin,** Tarnita, D., Nonlinear movement of human knee overground & on treadmill, Bulletin of the Transilvania University of Braşov, vol. 9(58) no. 2 - Special Issue Series I: Engineering Sciences, pp. 125-132, 2016.

[GEO2018] Geonea, I., Dumitru, N., Rosca, A.S., **Petcu Alin,** Ciurezu, L., Experimental Validation of an Exoskeleton for Motion Assistancen, Applied Mechanics and Materials, vol. 880, pp. 111-117, 2018.

[GSS2009] Sawicki, G.S., et al. A pneumatically powered knee-ankle-foot orthosis with myoelectric activation and inhibition, Journal of NeuroEngineering and Rehabilitation, vol. 6(23), 2009.

[BMM2013] Baig, M.M., Gholamhosseini, H., Smart health monitoring systems: an overview of design and modeling, J Med Syst, vol. 37(2), pp. 9898, 2013. [CAT2013] Catana, M., Tarnita, Daniela. Tarnita, D.N., Modeling, Simulation and Optimization of a Human Knee Orthotic Device, Applied Mechanics and Materials, vol. 371, pp. 549-553, 2013.

[CF2014] Casamassima, F., Ferrari, A., Milosevic, B., Ginis, P., Farella, E., Rocchi, L., A wearable system for gait training in subjects with Parkinson's disease. Sensors (Basel), vol. 14(4), pp. 6229–6246, 2014.

[CHO2013] Chowdhury, S., Kumar, N., Estimation of Forces and Moments of Lower Limb Joints from Kinematics Data and Inertial Properties of the Body by Using Inverse Dynamics Technique, Journal of Rehabilitation Robotics, pp. 93-98, 2013.

[CHY2013] Charlon, Y., Fourly, N., Campo, E., A telemetry system embedded in clothes for indoor localization and elderly health monitoring, Sensors (Basel), vol. 13(9), pp. 11728–11749, 2013.